Multiple-filtering-process for the Edge Detection of High-dynamic-range Images

Jing Li

A Thesis

in

The Department

of

Electrical and Computer Engineering

Presented in Partial Fulfillment of the Requirements
for the Degree of Master of Applied Science (Electrical and Computer Engineering) at
Concordia University
Montreal, Quebec, Canada

May 2009

Your file Votre référence
ISBN: 978-0-494-63114-0
Our file Notre référence
ISBN: 978-0-494-63114-0

ABSTRACT

Multiple-filtering-process for the Edge Detection of High-dynamic-range Images

Jing Li

Edge detection is a basic image processing operation usually used in the first stage of the complex image processing systems, such as restoration, and its quality has a direct effect on the performance of the systems. The extraction of correct edges from a noise-contaminated image or an image with severe deformation is a challenging task. The objective of the work of this thesis is to develop an edge detection method to extract effectively edge signals from the images with the edge information seriously damaged while being acquired in high dynamic range (HDR) scenes.

To achieve the objective, an edge detection method based on a multiple-high-pass-filtering process scheme has been proposed. Each of the filtering processes is designed to suit one of the signal deformation conditions, and is applied to the entire input image, instead of the designated regions, in order to spare the computation of image segmentation. A fusion process is then performed to merge the gradient maps generated by the multiple filtering processes into one. A detection procedure has been designed for a typical case of HDR images acquired with three different kinds of deformations due to the non-ideal characteristics of acquisition device.

Based on the study of the characteristics, three high-pass filtering processes are designed to generate gradient signals with different modulations. A simple selection algorithm is developed for an easy fusion process. The results of the simulation with different types of HDR images have shown that, compared to some of most commonly used detection processes, the proposed one leads to a better quality of edge signals from severely deformed HDR images.

Acknowledgements

I wish to express my sincere appreciation to my supervisor Dr. Chunyan Wang for her help and support during my study at Concordia University. Her insight, expertise and wealth of knowledge are invaluable to me. Without her help, I could not finish this study.

I would like to thank my friends: Shaofeng An, Jonathan Caso, Li Zhu, Yao Tang, Lin Du and Songsong Yang for their reviews of this thesis and helps to my life.

Finally, I would like to thank my family in China, and my relatives in North America, for all the love and support from them.

CONTENTS

List of Figures

List of Tables

List of Acronyms and Abbreviations

HDR	High dynamic range
HP	High-pass
LIP	Logarithm image processing
PLIP	Parameterized logarithm image processing
OI	Original image
FI	Filtered image
NFI	Normalized filtered image
SI	Selected image
EM	Edge map
PFOM	Pratt's figure of merit

List of Primary Symbols

Gx	Gradient value obtained by the horizontal direction mask of 1st order derivative edge detector
Gy	Gradient value obtained by the vertical direction mask of 1st order derivative edge detector
G	Ordinary gradient magnitude value
G_ϕ	Gradient value obtained by 1st order derivative edge detector in ϕ direction
ϕ	Direction information of gradient value
T	Threshold value
γ	Gamma value for gamma correction
I	Intensity value in the image
R	Reflectance
L	Illuminance
Φ	Scaling factor used in [12]
p_B, p_W	Probabilities of dark and bright pixels in [14]
t	Exposure time in [16]

s	Transform function from scene radiance to image irradiance
f	Transform function from image irradiance to image intensity or camera response function
n	The number of the multiple filtering processes
(x,y)	Pixel position in an image
I_{local}	Local intensity information
I_i	One of the pixel intensity in a small area
L, M, H	Low , median and high intensity conditions or sections
G_L, G_M, G_H	Adjusted gradient value obtained by the low, median and high intensity section adjusting function
G_N	Normalized G by dividing the maximum value of the whole gradient map
γ_L, γ_H	Gradient adjusting factor of low intensity and high section
G_{NL}, G_{NM}, G_{NH}	Normalized G_L, G_M, G_H
G_{good}	Selected normalized gradient value from G_{NL}, G_{NM} and G_{NH} by applying selection algorithm
FI_L, FI_M, FI_H	Filtered image obtained by the L, M and H intensity filtering processes
NFI_L, NFI_M, NFI_H	Normalized filtered image obtained from FI_L, FI_M, FI_H

SI_L, SI_M, SI_H	Selected image obtained under L, M and H intensity conditions
EM_L, EM_M, EM_H	Edge map obtained under L, M and H intensity sections
I_I	The number of ideal edge points in the image
I_F	The number of edge points found by the edge detector
I_N	The maximum of I_I and I_F
α	A scaling constant to adjust the penalty for offset edges
d_i	The distance of a found edge point to an ideal edge point

Chapter 1

Introduction

Digital image processing is widely used in many modern systems in our daily life. With the development of the technology, the image processing algorithms can be very computation-intensive to deal with sophisticate problems. Inside the most of image processing tasks, edge detection is often an essential operation.

Edge information in an image is found at the pixel positions where the image intensity gets discontinuities. This information is of important structural properties featuring the image. The edge detection is to extract it from a huge amount of the input image data. The extraction of correct edges from a noise-contaminated image or an image with severe deformation may not be an easy task. However, this information is indispensable in many image processes, such as image denoising, restoration and enhancement. Thus, an efficient edge detection method is needed to detect good edge information in the images acquired in various conditions.

In this chapter, a brief description of edge detection process is presented. Then the motivation and objective of the work of this thesis will be described. The scope and the organization of the thesis will also be presented.

1.1 Edge detection and the challenges

Since the edge information is about discontinuities in image amplitude, the differential detection is a widely used approach to the edge detection [1]. Its procedure is usually divided into two stages, as illustrated in Fig. 1.1. The first stage is to apply a differential process to the input image. The differential signal obtained in the first stage is then used to produce the edge map in the second stage. The computation in each stage needs to be designed to suit the conditions of the input image.

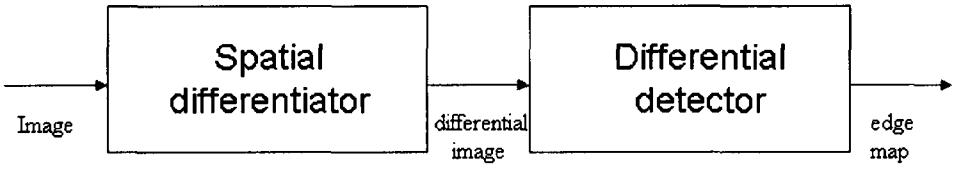

Fig. 1.1 Procedure of a differential edge detection process. [1]

In most of the edge detection tasks, the input images are contaminated with noise such as Gaussian noise, salt and pepper noise, or distorted by illumination variance. To extract the edge information from a noised image, one needs to investigate the characters of the noise and design the detecting process that is effective in filtering it out. There are a few approaches to such an edge extraction using the two-stage process shown in Fig. 1.1. One can add a stage of image enhancement before the differential detection. Also, the spatial differentiator can be designed to detect the signals of discontinuity attenuated by the noise. Furthermore, the processing of the differential signals can be

made to suit the noise condition and match the characteristics of the specifically designed differentiators.

In a kind of particular cases, the edge information is seriously degraded due to a non-ideal image acquisition process with under-exposure and over-exposure. This phenomenon is produced by the mismatched dynamic range of the cameras and the real scenes. The dynamic range is defined as the ratio between the smallest and largest detectable values of a changeable quantity. A real scene can have a very wide dynamic range, referred in literature as or high dynamic range (HDR). In practice, the dynamic range of image acquisition devices is usually much narrower than that of an HDR scene, which is illustrated in Fig. 1.2. Due to this mismatched condition, the image acquisition has to be done with under-exposure and/or over-exposure. In such a process, an HDR scene is thus often transformed into an image in which edge signals are damaged. To extract the edge information from such images, one can consider to compensate for the attenuation or to extract the edge signals in an intensity-dependent manner. For the compensation, a model of signal-attenuation has to be developed, which can be challenging. The extraction of the edge signals can also be a complex task. Either of them can be computation intensive.

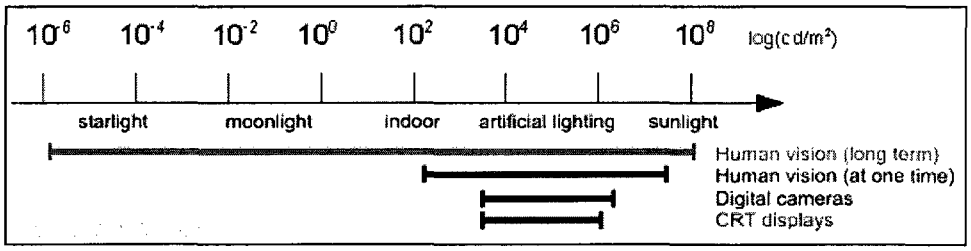

Fig. 1.2 Dynamic range of different optical and electrical devices. [2]

1.2 Motivation and objectives

In reality, it is impossible to find an acquisition device of which the dynamic range matches that of an HDR scene, for instance a landscape combining very bright parts such as the sky with clouds and dark parts under the shadow. Therefore, robust edge detection algorithms that are effective to edge-damaged images are needed. Furthermore, the implementation of such algorithms should not be difficult so that they can be integrated in various image processing systems, as the edge signal is used in almost all the processes.

The main objective of the work in this thesis is to develop an edge detection method. It should be effective to extract edge signal from an image in which the edge gradients are severely damaged by under and/or over-exposure during the acquisition of an HDR scene. It needs to yield high quality of edge signals that are to be used in image processes such as image denoising, restoration and enhancement. The computation procedure of this edge detection method should be simple to facilitate its applications in various image processing systems.

1.3 Scope and organization of this thesis

The work of this thesis focuses on extracting edge signals in the images captured under the HDR conditions. It will start with an investigation of the signal degradation under the unmatched dynamic range condition. Due to the complex phenomenon of the degradation, a procedure involving multiple filtering processes needs to be defined to

extract the edge signals under different conditions. These processes should result in appropriate gradient signals in different regions of the image. An edge map containing high quality signal will then be produced based on the gradient signals. Also, the results will be evaluated in both subjective and objective ways.

The thesis manuscript is organized as follows. In chapter 2, the background of edge detection is described. Some of the existing methods relevant to this work are also presented. Chapter 3 is dedicated to the description of the proposed edge detection method. The design of both the multiple filtering processes and the edge map generating process will be described in details. Chapter 4 presents the evaluation of the proposed method by subjective observations and objective measurements. The simulation results are also included. The work of the thesis and results are summarized in Chapter 5.

Chapter 2

Background

Since edge information plays a key role in many technologies, edge detection becomes very important in the processing of automatic vision operation system. The two stages of edge detection process mentioned in § 1.1 can be summarized as follows. Firstly, the level of the differential signals in the image is measured, such as gradient value. In normal cases, the real edge gradients have the higher level than noise signals. Secondly, the edge signals are determined by using a fixed threshold value. However, the accurate detection of edge is often not a straightforward task [3]. If the image contains many noise signals, a modified process needs to be introduced to detect the edge signals effectively. In some cases, images can be enhanced by some approaches such as [4] before operating edge detection. In [5] and [6], the modification is focused on designing spatial differentiators. In [7] and [8], a complex thresholding process is designed.

As mentioned previously, if images are captured under HDR scenes, the edge signals are attenuated or weakened in different intensity conditions. It is a typical edge deformation case. Besides the regular denoising process, some of the modified methods are proposed to against this deformation case. To study the background knowledge of the

edge detection and the principles of the modified methods can assist the design of the edge detection method in this thesis work.

In this chapter, some background knowledge of edge detection will be introduced in § 2.1. In § 2.2, some of the existing methods claimed that they can solve the problems in the images containing complex conditions will be presented. It includes the analysis of the advanced edge detection methods and some image enhancement methods related with the HDR problem.

2.1 Background of edge detection

Edge signals place in an image with strong intensity contrast, which often occurs at the locations representing to the object boundaries. In order to obtain the edge information, the following two steps need to be achieved: to characterize the edge signals; to judge the edge information based on the results from the first step. Concerning the first step, for example, the high gradient value is considered as one of the common characteristics of the edge signals. Moreover, if the gradients at one pixel position are calculated in different directions, the typical gradient value needs to be measured or decided by some different strategies, for instants, gradient magnitude or the maximum value from the values obtained in all the directions. Concerning the second step, the judgment is usually achieved by using a thresholding process performed on the results generated from the first step to decide which signals should be considered as the desirable real edges.

An ideal edge map, so called ground truth, can be obtained from the image under the noise free condition. For synthetic images or simple real images, it is relatively easy to

specify the ground truth. However, the desirable edge of a complicate real image is usually decided by the subjective evaluation. In general, the desirable edges should avoid following three major types of errors: (1) missing valid edge; (2) failure to localize edge point; (3) classification of noise fluctuations as edge points. These points should be considered in all the edge detection processes [1] [9]. As the background knowledge, two key points of the classical process will be presented.

2.1.1 Typical edge detection kernels

Since edge information of an image consists of mainly high frequencies, in general, it can be detected by applying high-pass (HP) frequency filters in the frequency domain (Fourier domain). In practice, this process is performed in the spatial domain to obtain gradients of the image by convolving the image with appropriate edge detectors which are actually some small kernels. The Sobel detector and the Laplacian detector are the two kinds of very popular classical edge detection kernels.

Sobel detector is a kind of typical 1st order derivative edge detectors. The mostly used horizontal and vertical Sobel kernels are shown in Fig. 2.1.

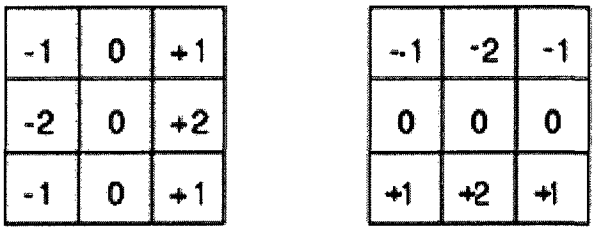

Fig. 2.1 Horizontal (left) and vertical (right) Sobel kernels.

The characters of the Sebol kernels are:

(a) Using the zero-including matrix to take the 1st order derivative. In spatial domain, the "0" between -1 and 1 allows the measurement contains more information when detecting the blurred edges; in frequency domain, this form gives suppression of high frequency terms and does not lead to a phase shift.

(b) Using one-dimensional version of a triangular filter to smooth the derivative results. In spatial domain, the "2" between two 1s provides a higher weight for the middle result; in frequency domain, this form does not exhibit phase reversal. [10][11]

Laplacian detector is another kind of popular detectors. It is an isotropic measure of the 2nd order derivative of images. Two commonly used kernels are shown in Fig. 2.2.

0	−1	0
−1	4	−1
0	−1	0

−1	−1	−1
−1	8	−1
−1	−1	−1

Fig. 2.2 Two Laplacian kernels (diagonal no considering and diagonal considering).

The first kernel consists of two 1-D 2nd derivative kernels in vertical and horizontal directions and the second one consists of four including two diagonal directions. They can be also considered as an all-pass filter (the core of the kernel) minus a low-pass filter (the neighbors around the core).

The results of the convoluting with Laplacian kernels are the isotropic 2nd order derivative values. The character of isotropic makes more benefits for detecting the single lines and the endpoints. Since Laplacian kernels are composed of 4 or 8 derivative sub-kernels [1 -1], the results are easily disturbed by noise signals. Therefore, in many

applications, Laplacian kernels have to be combined with Gaussian smooth kernels to reduce the detrimental effects of the noise. [10][11]

2.1.2 Edge signals judgment

The edge information has been extracted by the convolution process mentioned in § 2.1.1. However, the real edge signals have to been judged and separated from those temporary results. A lot of kernels can measure the gradient in different directions. For regular 1st order derivative kernel, for example, Sobel kernels with horizontal and vertical directions, the gradient magnitude value can be decided as the gradient value G which can stand for the edge signals. The maximum strategy is also a very common method to decide this value, especially for some kernels called compass edge detectors. In this process, for one pixel position, by measuring G_ϕ, where $G_\phi$represents the gradient value in ϕ direction, the maximum value of the group of G_ϕ is chosen as G. Considering the thresholding process, in a simple process, there is only one threshold value which is usually obtained from global characteristics of the image, for example, the global mean value. For the 2nd order class, edges are judged present if there is a significant spatial change in the polarity of the second derivative (zero-cross). [1]

2.2 Modified methods with adjustable parameters

In order to obtain high quality edge information in the images with noise signals, more information and parameters should be used to identify the real edges. In this work, intensity variance caused by HDR scenes is one kind of noise signal which makes edge

signals deformation in the image. Many modified methods are presented to detect edge information in such images. In this section, classical modified edge detection methods and several modern approaches which may solve the illumination problems in the images will be presented.

2.2.1 Classical modified edge detectors

Since classical edge detection process is sensitive with noise signal, some modified processes have been developed. For example, Canny detector and Gabor filter introduce denoise filter, orientation information into the process to reduce the effect of noise. Gabor filter may have high efficiency in some tasks when some pre-knowledge of the patterns has been known, such as finger print enhancement employed in [12] and feature detection in [13]. In many common applications, Canny edge detector is considered as a effective edge detector. It is used and modified in many image processing tasks reported in many papers, such as [14]-[16]. This detector named after John Canny, who described this method in 1986 [17], was designed to meet three criteria for edge detection:

1. Low error rate of detection (false and lost edge);
2. Localization of edges (Minimum distance between actual edges and detected edges);
3. Single response (thinning process).[18]

Canny detector uses Gaussian smooth to reduce the noise in the first stage, and then measures the gradient magnitude values and orientations by using classical 1st derivative edge detector, for example Sobel. The next step is non-maximum suppression. Assuming that one pixel has a direction ϕ, to be considered as an edge pixel, this pixel must have a

greater magnitude than its neighbors in direction ϕ. In the thresholding process, Canny edge detector introduces a tracking process controlled by two thresholds: upper threshold T_1 and lower threshold T_2, with $T_1 > T_2$. Tracking can only begin at a point on a ridge higher than T_1. Tracking then continues in both directions out from that point until the height of the ridge falls below T_2. This process helps to ensure that noisy edges are not broken up into multiple edge fragments. [19]

Although Canny modified almost all the steps of the edge detecting process, which may absolutely improve performance of the detection, it is still have some problems to preserve the edge signals in HDR images, which means the performance still can be improved, and meanwhile the calculation complex might be reduced.

In conclusion, catching the information which can represent the edges and judging the edge signals are the two main steps in the edge detection process. However, to obtain the accurate edge signals in an image which involves complicate conditions, no less than this work, the modified adjustable process has to be employed.

2.2.2 Relevant approaches related to the HDR problem

In this thesis work, the edge information in images captured in HDR scenes needs to be detected accurately. As the edge strength changes with the background illumination, the classical edge detection process is difficult to sense this changing and it cannot detect edges in a discriminated manner. Hence, the "Fault edge" and "edge lost" will be shown in the edge map. To solve the problem, some of the simple enhancement models which can adjust the illumination or contrast are developed, for example, γ adjusting model. These methods provide a fixed transform function to enhance the image. However, these

adjusting processes are too simple to cover the complex deformation and illumination conditions. To receive better quality, different functions have to be applied to the regions with different conditions. Since the complex conditions of the signal degradation in the HDR image, to enhance and analyze such images are not easy tasks, for instance, the algorithms and circuits presented in [20]-[23]. In this subchapter, some edge detection approaches that can solve this sort of the problems are presented, and some tasks related with HDR image visualization are discussed as well.

Some of the methods employ a modified edge gradient algorithm. For example, in [24], authors proposed a new model called Logarithm Image Processing Model (LIP Model). They redefined the "+" and "×" functions for measuring the gradient values. This model is improved by Guany Deng in [25] by combining with Sobel detector. The authors claimed that: "the output of the LIP-Sobel operator is only dependent on the reflectance or transmittance of the scene, and not on locally small changes in illumination. [25]" Recently, this method is modified again in [26] and is used to image enhancement. In this method, authors proposed a modified LIP-Sobel detector called Parameterized LIP-Sobel (PLIP-Sobel). Image is enhanced by two key components: edge map obtained by using four-direction LIP-Sobel detectors and local mean values of the original image. "The LIP-Sobel detector detection technique is robust in slow changing illumination conditions. [25]" However, since this model is still established based on logarithmical adjusting, it may be limited in some complex edge attenuation conditions.

Since a simple adjusting function cannot solve the HDR problem effectively, in some of the works, authors introduce a complicated function to cover all the conditions in the whole image. A gradient magnitude adjusting method is proposed in [27] to enhance the

images with the HDR problem. This process is based on a model of an intensity and luminance variance: $I(x,y) = R(x,y) \cdot L(x,y)$, where *I(x,y)* is the intensity of a pixel at position *(x,y)* in the image. *R(x,y)* is the reflectance and *L(x,y)* is the background illuminance at point *(x,y)* [27]. This process is a modified homomorphic filtering process. Firstly, to avoid illuminance component, before measuring the gradient values, *I(x,y)* is transformed into logarithmic domain. The gradient magnitude values $\|\nabla H_k(x,y)\|$ are measured in log-domain, and then they are adjusted by the two other parameters α and β to generate a scaling factor $\Phi(x, y)$ at each position of the image. Finally, the enhanced images are obtained by the exponential function. The processing procedure is illustrated in Fig. 2.3.

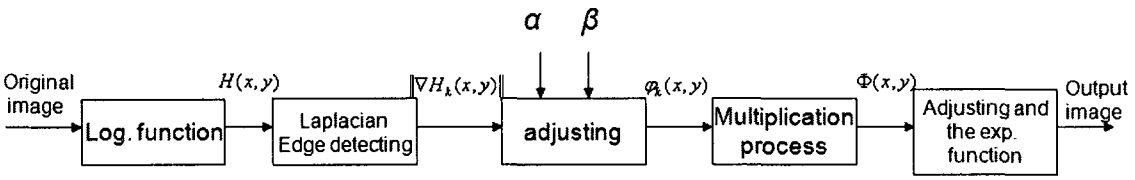

Fig. 2.3 Processing procedure in [27].

Similarly, authors proposed an equation in [28] as a vision model which can combine with some classical edge detectors to detect edge signals in the image under the complicated illumination conditions.

The main feature of this kind of approaches is that the adjusting function can be built perfectly to satisfy the all the conditions in the image. Each point of the image is adjusted accurately. However, the adjusting function is very complicated. Usually, it cannot be achieved on one computation stage. The parameters used in the function are also measured difficultly. Therefore, the computation of the whole process is very heavy.

In order to simplify the adjusting process, some of the methods which use a group of processes instead of a single complicated process are proposed. The single adjusting function is separated into several pieces which approximately equal to the complicated nonlinear transform function. In these approaches, the image is considered to be composed of many regions. The regions which have the same character will be processed by one simple adjusting function designed for this character. For an image involving complex conditions, several functions should be designed. This approach can be called as "multiple processes" approach.

The straightforward way of using this approach is that the image is separated into several segments according to some certain characters, and then each segment is passed through a transform function. In the end, all the processed segments are combined together to obtain the results.

This approach is used in many contrast enhancement tasks. For example, the image is segmented into three segments, dark, median and bright by two threshold values of the intensity in [29]. These threshold values are measured by a histogram-based segmentation algorithm. For example, if we want to obtain the threshold value T between dark and bright segments, to make the entropy: $H = -\sum_{i=0}^{T} p_B \log p_B - \sum_{i=T}^{255} p_W \log p_W$ reaches the maximum value, where p_B and p_W represent the probabilities of dark and bright pixels. After the segmentation process, luminance in each segment is adjusted by a contrast adjusting equation in which parameters are acquired from each segment. This processing procedure is illustrated in Fig. 2.4.

The process in [30] is similar as [29], a human vision algorithm is introduced to be the segmentation algorithm, each of the segment is pass through a enhancement process in which the parameters are different with other segments. In the end, all the segments are unionized into a complete image.

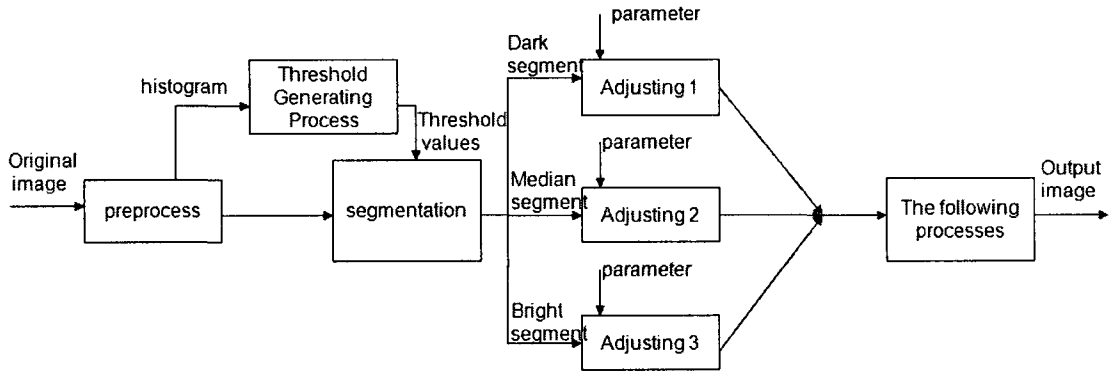

Fig. 2.4 Processing procedure in [29].

In general, in this scheme of the multiple processes approach, firstly, a good segmentation algorithm has to be designed. After applying the segmentation process, each transforming or adjusting function is applied to the corresponding segment. The last step is to combine all the processed segments into a complete result.

In some cases, to design a perfect segmentation algorithm is very difficult. Identifying the real boundaries of the regions may not be an easy task. Insufficient quality of the segmentation can result in some negative effects such as visible artifacts. In some approaches, supplementary process is developed to reduce the artifacts, such as the multi-scale filtering presented in [31]. Therefore, the segmentation must be designed carefully to make sure that the outputs of the multiple processes are perfect. It leads heavy computation on the segmentation process in the beginning and in the combination

process in the end. Because of this problem, another scheme of the multiple processes system is proposed. In this scheme, a group of the processes is applied to the entire image to generate a set of the processed images respectively, and then by using a fusion algorithm, the desirable results are obtained from the group of the processed images. Many HDR image compression methods employ this scheme. It is because that the pictures captured in different exposure times maintain all the details in the whole dynamic range of the real scene. The multiple-exposure-process can be considered as a group of transforming processes.

In [32], authors presented a control system that assists digital camera to capture the HDR scene. First, the camera captures an image under the default exposure time t_1, and then based on this default image, other two exposure times t_2 and t_3 are estimated, and are used to capture other two images. Finally, the pixel intensities in the output image are computed from the weight average of those in the three images by using a simple algorithm. This process is illustrated in Fig. 2.5.

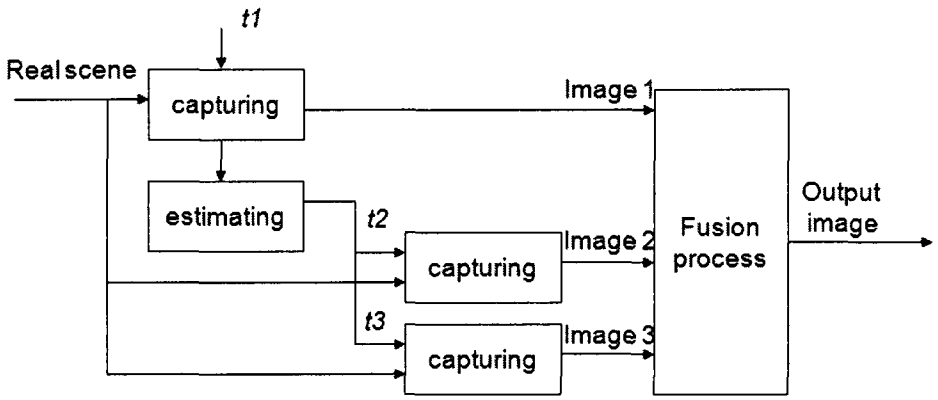

Fig. 2.5 Flow chart of the image capturing process proposed in [32].

Another example is the multiple exposure time images synthesizing process proposed in [33]. The real scene is captured by a camera with two exposure times. One is

for preserving the details in dark illumination condition and the other one is for that in the bright illumination condition. Both of them are passed through Sobel edge operators to obtain the gradient magnitude values. The desirable gradient values are selected and combined from those two gradient maps. Finally, the synthesized image can be reconstructed. The process is illustrated in Fig. 2.6.

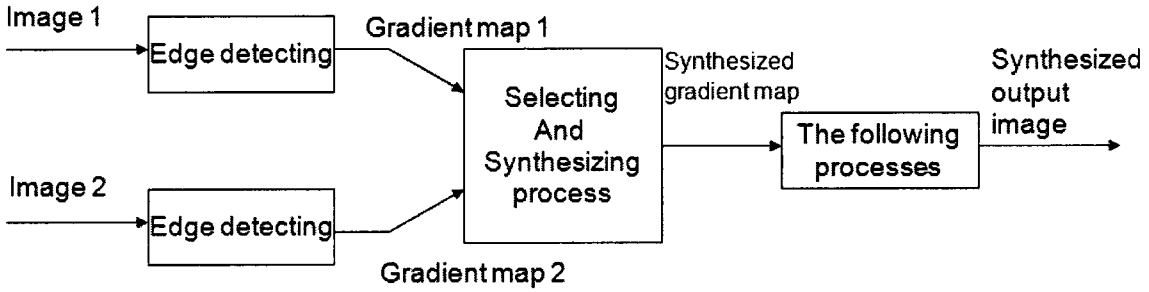

Fig. 2.6 Synthesizing process in [33].

In general, this scheme of the multiple processes includes two parts: to apply a group of transforming functions, for example same kind of the filtering processes, to the entire image to obtain several processed images respectively; to design a fusion algorithm in which some parameters obtained from those processed images are needed. The final results can be measured by using this algorithm. Although each process is applied to some regions of the image, the whole process does not involve an explicit segmentation process. The segmentation process is replaced by the fusion process. In some of the image processing tasks, since the fusion process is operated on the processed images, the algorithm may not be complicated. Therefore, the complex of the computation of the whole process may be reduced. The main scheme of this approach can be displayed as the following process shown in Fig. 2.7.

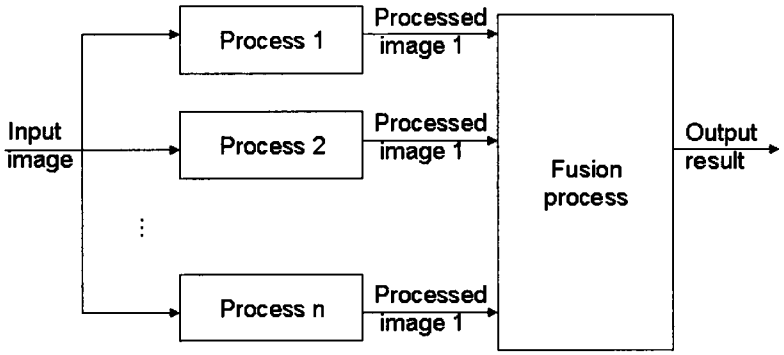

Fig. 2.7 Scheme of the multiple processes without explicit segmentation process.

2.3 Summary

The objective of this thesis work is to detect the edge information in the image captured in HDR scenes. In this chapter, firstly, the key steps of the classical edge detection are discussed. The edge kernels and thresholding process should be designed based on the different applications. Since the classical edge detection process employs fixed parameters to detect edge information, it can only be used in simple tasks. In complex cases, due to the variety of the conditions in the image, classical edge detection process cannot extract the edge signal effectively. Therefore, modified processes introducing adjustable parameters are needed. Some of the works are presented in § 2.2, including classical modified edge detection processes and several latest approaches that may solve the problems caused by illumination variance in the image.

In order to reduce the complex of the transforming or adjusting function, the multiple processes adopted in [29]-[33] is introduced. In the multiple processes, different regions may receive different adjusting function. In [29] and [30], authors introduced segmentation process to divide the image before applying the multiple processes. In some

other works, another structure of multiple processes without explicit segmentation which are adopted in [32] and [33] is presented.

In the next chapter, the proposed edge detection method will be presented. Based on the particularities of detecting edge signals in HDR image, the design principles will be discussed and the structure of the methods will be introduced and analyzed, and then each part of the proposed process will be presented in detail.

Chapter 3

Procedure of the Proposed Edge Detection

As described in Chapter 2, edge detection is a basic process in image processing and it can however be complex due to the noise presence or difficulties occurred in the image acquisition. The objective of the work in this thesis is to detect the edges in an image of a high dynamic range (HDR) scene. In such an image, the edge gradients may be severely damaged dun to the deformation by the acquisition process. The complexity of the deformation is related to a complicated manner of the attenuations of the edge signals. A simple high-pass filter can only effectively detect edge gradients under one particular condition. The case of HDR image is often processed by using a complicated filtering function which requires a large amount of computation. Another approach to handle with the images with HDR problem is to apply multiple filtering processes, i.e. a set of simple functions, each of which is designed to adapt to a particular deformation condition. This approach may result in an easier implementation of the process.

The multiple filtering processes for the HDR image processing can be used in two different schemes mentioned in the Chapter 2. The first one is to segment the input image into different sections according to different conditions, and then apply each of the processes in the appropriate section. It should be noted that, in an image acquired in a real

scene, the signal varies over the space in a continuous manner. It would be a complex computation task to define precisely the boundary pixels between two regions. Inaccurate segmentation can produce visible artifacts in the processed images. To avoid the computation of such a complex segmentation, one needs to find an alterative approach. It is often the case in signal processing that some features or characters are easier to be identified in one domain, e.g. the frequency domain, than in another one, e.g. time, or space in case of still images. Therefore, multiple filtering processes can be applied to the same image, resulting in multiple images in filtered domains, and then those images are merged to produce final result. If the merging algorithm is made to be simple and effective, the edge detection method in this case can be designed simpler and better in the terms of quality and facility of the implementation. In this chapter, in main procedure of the edge detection by using multiple processes without segmentation is described. The details of each part of the process are also presented.

3.1 Description of the structure of the procedure

The non-segmentation multiple filtering processes can be depicted as the scheme shown in Fig. 3.1. There are n simple filtering processes, each of which aims at detecting edge gradients in a kind of regions, and applied to the entire original acquired image (*OI*). Thus, n filtered images (*FIs*) are then generated. A selection algorithm needs to be designed to combine these *FI*s to form a complete image.

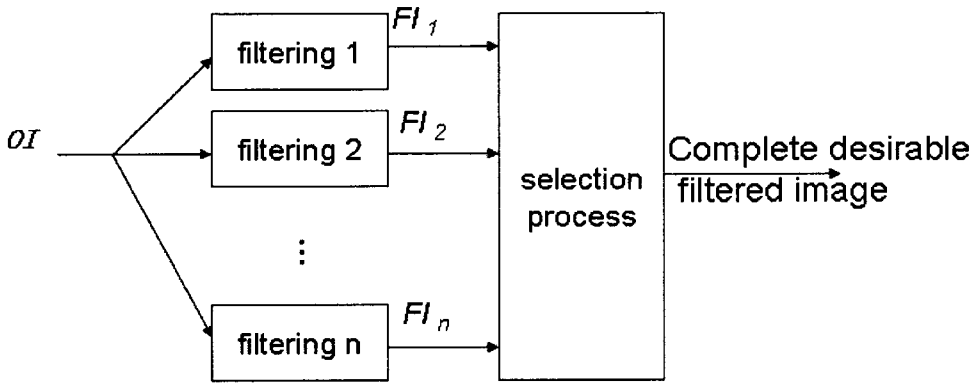

Fig. 3.1 Scheme of a multiple filtering processes without image segmentation.

The original image is composed of many regions. The signals in some regions may be acquired under a particular illumination condition. These regions that may not be adjacent are grouped as one section. Each filtering process is designed to suit the condition of a section. Therefore, in each *FI*, only the pixels in these regions, considered as "matched regions", can receive the correct results from this filtering process, and the rest parts of the *FI* are the "unmatched regions". As the pixels in different sections receive different filtering processes, they are transformed to be more easily identified by their regions than in their original domain. The selection algorithm can be designed to distinguish the matched regions from unmatched ones. In this way, "unmatched regions" will be filtered out by the selection process from all the *FI*s, and only the "matched regions" are preserved to generate a complete filtered image.

Let us have analysis of this process in the pixel level. Of all the *FI*s, at a particular pixel position, n values resulting from n filtering processes are received. However, only one of them is the "good result" produced by the matched filtering process. It should have distinguished characters to be identified in the selection process. In other words, the selection criteria should be established based on the analysis results of these characters.

They can be described by a mathematic model which is used to develop the selection algorithm to identify the desirable result from the n values. The selection is processed in the pixel level, and the boundaries of all the regions are defined automatically pixel by pixel.

Based on the scheme shown in Fig. 3.1, the main structure of the proposed edge detection method can be shown in Fig. 3.2. The multiple filtering processes in this case are a set of differential computation processes, and each of them is to match one kind of the edge signals attenuation. A group of the filtered images (*FI*s) are generated by the HP filtering processes. In this design, each of the *FI*s is a gradient map in which only the pixels in the matched section have their gradients enhanced. Like most of the edge detections, the edge map is obtained by binarizing the gradient signal at each pixel position with a threshold. A selection process is applied to pick up the good gradient signal from the n values produced by the n *FI*s. In this procedure of edge detection method, the fusion process is in fact composed of two parts: the selection process and the thresholding process.

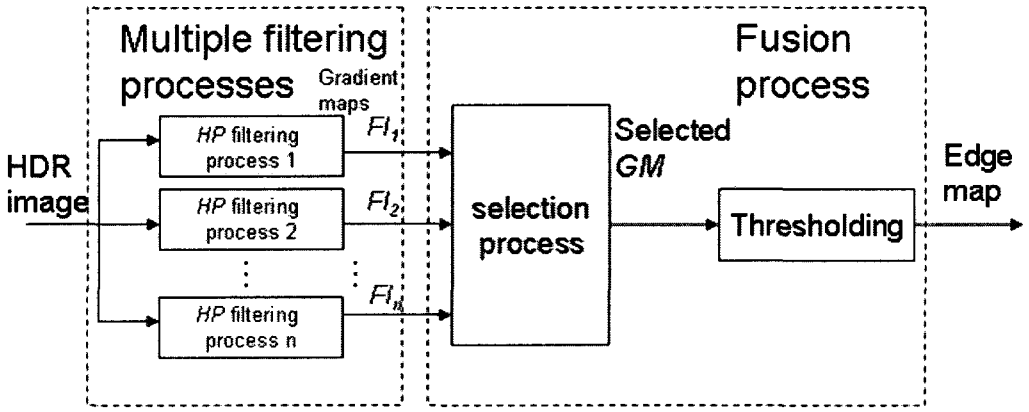

Fig. 3.2 Structure of proposed edge detection method.

The proposed edge detection method does not include any segmentation. One does not wish the fusion process complicated. The simplicity of the whole process is related very much to design of the filtering and selection processes which will be presented in detail in the following sub-chapters.

3.2 Design of the filtering processes

This work aims at edge detection of images of HDR scenes. The images are usually acquired by image sensors with narrow dynamic range and by single exposure. The image contrast that is related to edge signals may be damaged by either over or under exposure conditions. In order to enhance or to restore the signals, the characteristics of the image acquisition devices need to be investigated. The studies of the features of edge signal attenuation is based on the investigation results, and then the suitable filtering processes can be designed.

3.2.1 Analysis of the edge attenuations

The signal of an HDR scene can vary over a very wide range, e.g. 5 decades or more, which greatly exceeds the range of the linear operation of image sensors. The images captured in the HDR scenes usually contain over and under exposure regions, in which the contrasts of the objects are very low with respect to their background signal level. A diagram showing how the real scene radiance is transformed to image brightness is presented in Fig. 3.3 [34]. This diagram illustrates that the original scene is turned into an image with a non-linear deformation. The non-linearity is usually given by the image

sensor, or camera; and a good study of this non-linearity is necessary to design a process to recover the signal.

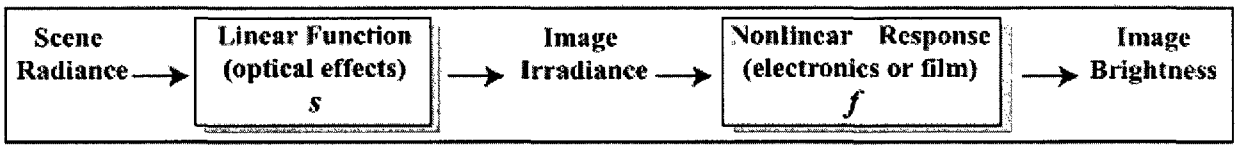

Fig. 3.3 Diagram of the transformation from scene radiance to image brightness [34].

In [34], the characterization of a good number of cameras and films are reported, and some of the results are shown in Fig. 3.4(a). These results confirm that the characteristics of a camera response have the property of signal compression at a high irradiance range and of expansion at a low irradiance range. The characteristic curve shown in Fig. 3.4(b) is obtained by combining some curves shown in Fig. 3.4 (a). Similar results of the characterization of other image acquisition devices have been reported in [35] and [36].

In an ideal case, the signal in form of optical irradiance is logarithmically compressed while being transformed to the gray level signal of an image. In practice, however, the characteristic of an image sensor is not ideally logarithmical. In a real acquisition process, if the image is acquired by a single exposure, in case of an HDR scene, the exposure time is usually set to suit the median irradiance. Since the dynamic range of the sensor is much narrower than that of the scene, the following deformation will occur.

- For the part of low irradiance of the scene, the signal is acquired with under-exposure. Due to the insufficient number of photons received by the sensor

at too short-exposure time, both the amplitude of the variations of the intensity signals and the level of the background are lower than they should be. The lower the irradiance, the smaller the gradients of the edges may be obtained. In this case, if G represents the edge signal, I_{local} represents the intensity signal at this position, one will have $\frac{dG}{dI_{local}} > 0$.

- Due to the saturation of the image sensors, a signal of high irradiance is transformed into a gray level signal with a compression more than that of the logarithmical one. Moreover, the higher the irradiance background, the stronger compression. Contrary to the case of the low intensity, in this case, we have $\frac{dG}{dI_{local}} < 0$.

By the above analysis, one can see that the signal deformation in an image, acquired with a sensor or a camera with a much narrower dynamic range than that of a real scene, is rather complex. To detect the edge signal of such an image, one need to restore the damaged edge gradients with the filters specifically designed to deal with the different conditions.

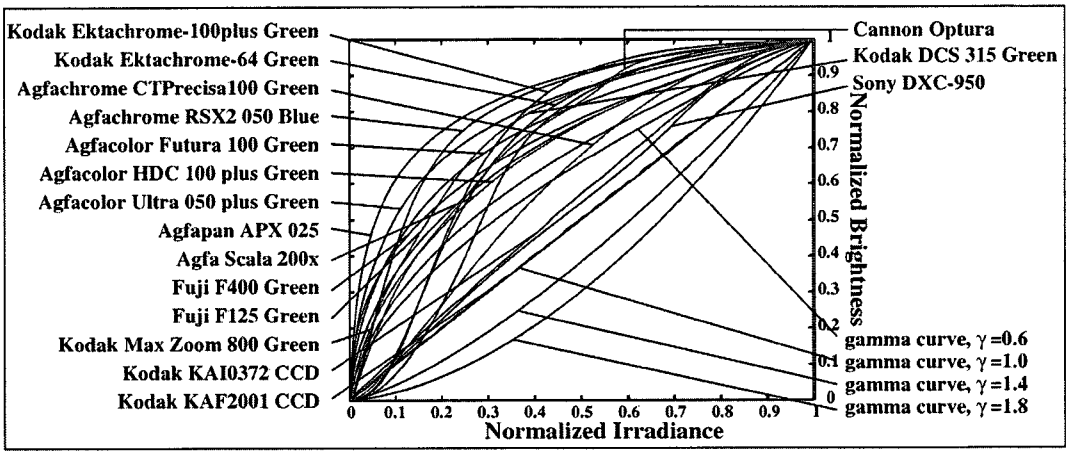

(a)

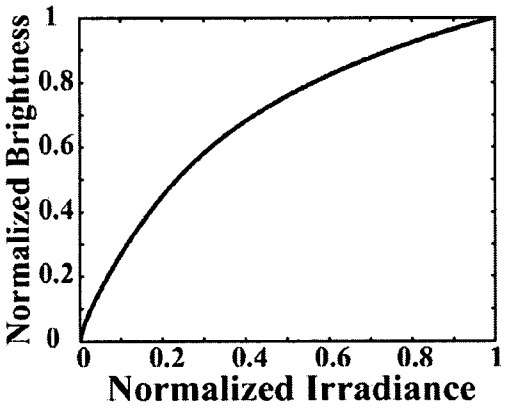

(b)

Fig. 3.4 (a) Responses of real films, digital cameras to the irradiance. The y-axis represents the normalized brightness or intensity of the image. (b) Combined characteristics of response. [34]

3.2.2 Design of the multiple filtering processes

As described in § 3.1, instead of a complex filter, a set of filters are to be used in the proposed edge detection method. Each of the filters should be designed for one section of the input image. One section may be composed of a number of non-adjacent

regions where the intensity condition is likely to be the same. Due to the problem, such as the under-exposure in the low intensity regions, the gradients of the real edges may be attenuated to be smaller than the non-edge ones in a section. The objective of the filtering is to enhance the edge gradients within the section in order to remove the effects of edge attenuation. In other words, the filtering function should provide a stronger gain to the more-attenuated gradients to distinguish the edge ones from the non-edge ones and a weaker gain to the less-attenuated.

Each of the filtering functions is the proposal detection method involves the gradient calculation and the modulation of the gradient value by the intensity signal in the neighborhood. The former can be of one of the commonly used differential operators, such as Sobel. The latter is determined by the way how the gradient signal is attenuated in a particular section. For the work presented in the thesis, the input image is assumed to be composed of three sections and thus three filtering process are to be designed.

(1) In the section where the intensity is the lowest, the edge and background signals are both weakened due to the under-exposure acquisition as described in § 3.2.1. It should also be noted that the amplitude of edge gradient in the lower end of the intensity range of this section is likely to be smaller than non-edge at the higher end. The gradients in the section are signal-dependent in such a way that the gradients attenuated more in a lower part of the intensity range. In order to remove the factor of the attenuation, the gradients modulation should also be signal-dependent. Let G_L be the modulated gradient in the low-intensity range. It should be inversely proportional to the local intensity. If G is the ordinary gradient value obtained by a classical differential process, we make:

$$G_L = G / \sum_{i=1}^{m} I_i^{\gamma_L} \tag{1}$$

where $\sum_{i=1}^{m} I_i^{\gamma_L}$ is the level of the local intensity as I_i, $i = 1, 2, 3\ldots, m$, is the signal in the neighborhood of m pixels. The factor γ_L, $0 < \gamma_L < 1$, is determined by the sensor device used in the acquisition. In many cases, $\gamma_L = 0.5$.

(2) The gradients in the highest intensity range are also attenuated in a signal-dependent manner. However, the cause of the attenuation is different. When the high irradiance signal is acquired, the signal variance in a higher level is weakened more than those in a lower level within the same range, i.e. the same section, which results in $\frac{dG}{dI_{local}} < 0$ as described in § 3.2.1. Since the ordinary gradient G is attenuated more if the intensity increases, in order to remove this kind of attenuation, G_H, the modulated gradient in the high intensity range should be proportional to the local intensity or the compensation. Therefore, we have:

$$G_H = G \cdot \sum_{i=1}^{m} I_i^{\gamma_H} \tag{2}$$

where $\gamma_H = 1$, in many cases.

(3) In third section, called the median section, the pixel signals are in the median intensity range. The variations of the gradients in this section are considered almost intensity independent. Therefore, if we have G_M represents the gradient in this section, we have

$$G_M = G \tag{3}$$

In summary, as the image is divided, according to the intensity levels, into three sections, three filtering processes are designed. Aiming at removing the factor of edge

gradient degradation caused by different non-ideal elements in the image acquisition, each of the filtering processes involves specific gradient modulation. As described previously in § 3.1, each of the filtering processes is to be applied to the input image, generates three filtered images. In the following sub-chapter, both the selection algorithm to identify the good pixels and the fusion process to produce a completed edge map will be presented.

3.3 Design of the fusion process

The fusion process is to produce a complete edge map from the filtered images generated by the multiple filtering processes. As each *FI* contains so called "good" and "bad" results from matched and unmatched filtering processes, respectively, a selection algorithm is needed to filter out the bad ones. Also, to complete the edge detection, a thresholding must be involved. Both selection algorithm and the thresholding are presented in this sub-chapter.

3.3.1 Selection process

As described in the preceding sub-chapter, each of the filtering processes is designed to suit the deformation condition of one particular section. Thus, in each of the *FI*s, the likely edge gradients in the section are compensated. As the same filtering process is also applied to the pixels of the other sections in the same image, the gradients of these pixels will be modulated in an inappropriate way and somehow suppressed. Hence, in this *FI*

the pixels of the matched section are likely to have their modulated gradients greater than those of the rest of the *FI*. However, as the three filtering processes are designed differently, statistically the range of gradient magnitude of one *FI* is very different from that of another *FI*. One can not distinguish a good result in one *FI* from a bad result in another simply by comparing their magnitudes. Thus, pixel gradients need to be adjusted to facilitate the identification of the good filtering results. This adjustment is the first part of the selection process. The selection criteria are set up according to natures of the adjusted gradients at each pixel position.

The gradients are modulated by the filtering processes with the factor of the local intensity and therefore they are signal-dependent. However, as the way of modulation is different from one filtering process to another, the magnitudes of the three modulated gradients at the same pixel position provided by the three *FI*s are very different. To identify which one of the three is the good one, each of them needs to be adjusted by a signal-and-process-dependent "normalization" factor. In this design, all the modulated gradients in each *FI* should be normalized by a factor generated from the gradients in the same *FI*. This factor for each *FI* is the maximum modulated gradient found in the *FI*. In this way, the gradient values are normalized to be between 0 and 1, and needless to say that the good results can still be distinguished from bad ones in the same map. By such normalization, at each pixel position among the three normalized gradients from the three *FI*s, the good one must be greater than the two. Thus, the criteria of the selection are about the magnitude comparison of the normalized gradients at each pixel position.

Let G_{NL}, G_{NM} and G_{NH} be the normalized G_L, G_M, and G_H, respectively. At a given pixel position *(x,y)*, the normalized values are given by the follow equations:

For the low intensity section:

$$G_{NL}(x,y)=G_L(x,y)/Max\{G_L\}=\frac{G(x,y)}{\sum I_i(x,y)^{\gamma_L}}/Max\{G_L\} \tag{4}$$

For the median intensity section:

$$G_{NM}(x,y)=G(x,y)/Max\{G_M\} \tag{5}$$

For the high intensity section:

$$G_{NH}(x,y)=G_H(x,y)/Max\{G_H\}=G(x,y)\cdot\sum I_i(x,y)^{\gamma_H}/Max\{G_H\} \tag{6}$$

At each pixel position, if G_{good} represents the good result selected from the three normalized gradient values, we have

$$G_{good}(x,y)=Max\{G_{NL}(x,y),G_{NM}(x,y),G_{NH}(x,y)\} \tag{7}$$

as the selection criteria.

The characteristics of the normalized gradients G_{NL} G_{NM} and G_{NH} versus the local intensity information I_{local} *(x,y)* at a given pixel position *(x,y)* are plotted and shown in Fig. 3.5. The calculation is done with $G(x,y)=10$ obtained with one kind of 1st derivative differential operator, $\gamma_L=0.5$ and $\gamma_H=1$ and I_{local} *(x,y)* being average intensity in the 3x3 pixel neighborhood calculated with the weights depending on the differential kernels.

The plot shown in Fig. 3.5 illustrates that when the intensity is low, G_{NL} is the highest among the three normalized gradients. Similarly, in the range of the high intensity, G_{NH} is the highest one. Furthermore, in the median range, G_{NM} is greater than other two as

expected. The characteristics of the normalized gradients produce a good agreement with the equation (7), the results of analysis for the selection algorithm.

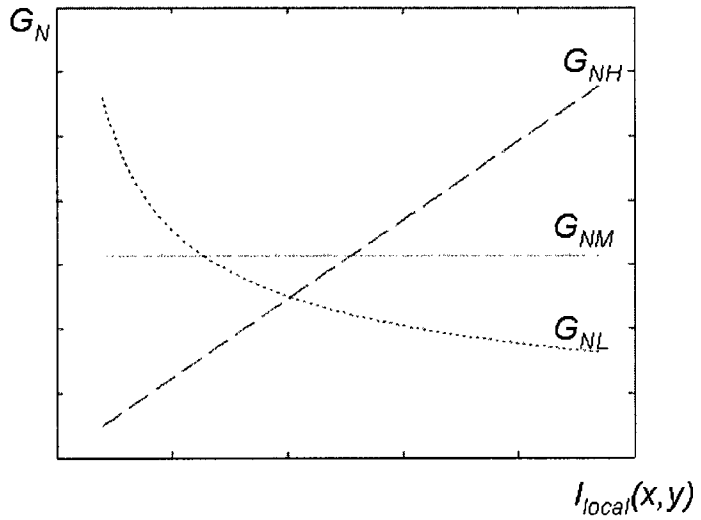

Fig. 3.5 Normalized gradients generated by the three filtering processes versus the average level of the original pixel signals in the 3x3 neighborhood at a given position *(x,y)*. The dotted curve is of G_{NL}; the solid one of G_{NM}; the dashed one of G_{NH}. The curves are obtained with $G(x, y) = 10$.

Once the pixel selection is done, all the "good" results generated from the three processes make a complete normalized gradient map. The following step is to perform binarization in this complete image.

3.3.2 Thresholding

In this design of the edge detection process, the efforts are on the generating the good gradients from the damaged image signals. Hence, the thresholding process is relatively simple. In this stage, the objective is to identify the edge gradients from non-edge ones. As the normalized gradients in the different sections are produced by the

different modulations and adjusted with the different normalization factors, it is important to determine the threshold in each section with the gradient information statistically extracted from the section. In this design, the threshold value in each section is determined by the mean value of its normalized gradients. The results of the thresholding in the three sections make to a complete edge map.

3.4 Procedure applying the proposed edge detection method

The proposed method described in the preceding part of the chapter can be implemented in the flow charter shown in Fig. 3.6. It proceeds as follows:

(1) The original image is usually pre-processed by a smoothing filter;

(2) The result of step (1) is processed by the filters involving classical gradients specified in § 3.2.2;

(3) The pixels in each *FI* are adjusted to generate the normalized *FI* images NFI_L, NFI_M and NFI_H;

(4) At every pixel position, the local normalized gradient is compared to the other two, from the other *NFI*s respectively. For each *NFI*, if the local one is the maximum among the three, it will be kept at this position. Otherwise, the pixel value at this position will be replaced by zero. The outputs of this stage are the images SI_L, SI_M and SI_H, with *SI*s standing for the selected images;

(5) A thresholding is applied to each *SI*. The threshold value is determined by the mean value of all the non-zero pixels and applied to this *SI* to perform

binarization. The complete edge map is combined by three edge maps: EM_L, EM_M and EM_H.

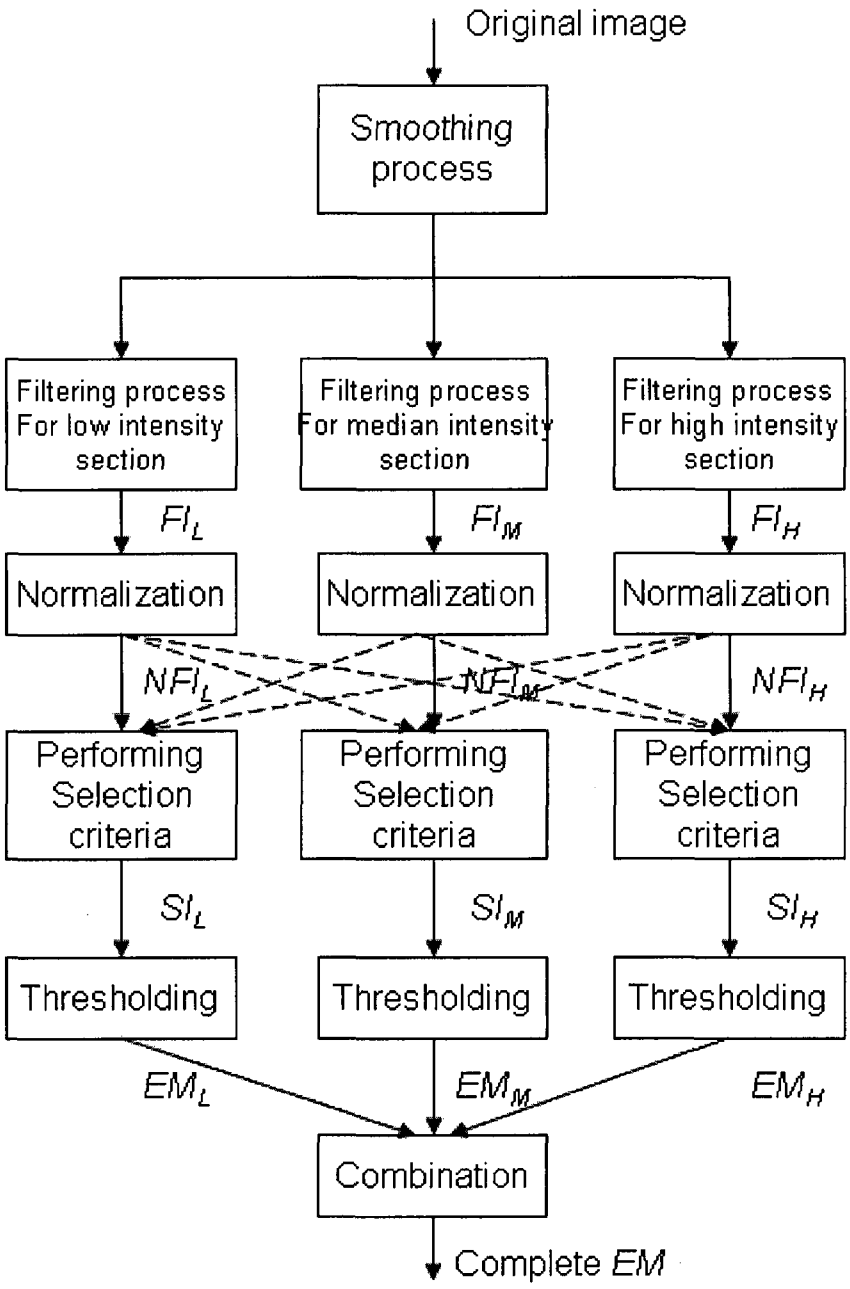

Fig. 3.6 Procedure implementing the proposed edge detection method.

It should be noted that the proposed method can be implemented in a flow charter different from that shown in Fig. 3.6. Each implementation procedure can result in different computation time if it is for a software program, or hardware consumption in case of circuit.

3.5 Summary

In this chapter, a procedure for the edge detection of the images acquired in HDR scenes has been proposed. It is based on a scheme of multiple filtering processes. In order to avoid complex computation of precise segmentations, each of the processes is applied to the entire image and several filtered images are then merged by means of a simple fusion process to create a complete edge map.

As the edge detection targets the images of HDR scenes, the characters of the image signal deformation due to the narrow dynamic range of the acquisition devices have been studied. Based on the results of this study, three filtering processes are designed to match three image sections corresponding to the different intensity conditions, respectively. Each filtering is of the modulated-gradients operation. The application of the three processes results in three filtered images. In the fusion process, the selection is done at each pixel position to identify the good modulated gradient, i.e. the one generated by the matched process. To facilitate the selections, the good modulated-gradients are adjusted in such a way that the magnitude of these gradients will be significantly larger than those by the non-matched ones. The selection process generates a normalized gradient map consisting of all the good gradients. A thresholding is then applied to the gradient map to

produce a complete edge map. The threshold in each section is determined by the gradient information extracted in the section.

This edge detection method aims at simplify the complex edge detection computation requiring multiple filtering processes by removing the segmentation. To achieve the objective, the selection process should not be computation intensive. In this design, the selection process is very simple considering the three different intensity conditions that result in the three kinds of signal deformations. For a case with more complex input signals, the computation for the selection may be less simple, and needs more parameters for the decision. However, it can still be made much simpler than the computation for a good segmentation of a complex image.

In the next chapter, the simulations with different types of HDR images are described and the analysis of the results is presented for the evaluation of its effectiveness.

Chapter 4

Simulation Results and Evaluation

The proposed edge detection method has been described in Chapter 3. In this chapter, the simulation results and an assessment of the effectiveness of the proposed method are presented.

As the proposed method aims at the edge detection of HDR images with damaged contrast signals, the images having such characters are used in the simulations. The results are then compared with those produced by some of the most commonly used algorithms. The assessment is done by subjective observation and objective measurements.

The first part of the chapter is to describe the simulation process. The subjective assessment is presented with the simulation results of the images acquired under different HDR scenes. The same images are also used for the objective measurements, which can be found in the last section.

4.1 Description of the simulation process

The simulation of the proposed edge detection method is done by using the Matlab tool. The program is written based on the computation procedure shown in Fig. 3.6. For

the convenience of readers, it is also illustrated in Fig. 4.1. The Gaussian smoothing operator sized 5x5 pixels with $\sigma = 1$ is used in the procedure. In the three filtering processes, the Sobel kernels are chosen for the ordinary gradient operation, and the parameters of $\gamma_L = 0.5$ and $\gamma_H = 1$ for the modulations. In the stage of the thresholding, the threshold to be applied in each of the three *SI*s, i.e. selected images, is the mean value of the normalized gradients in the *SI*.

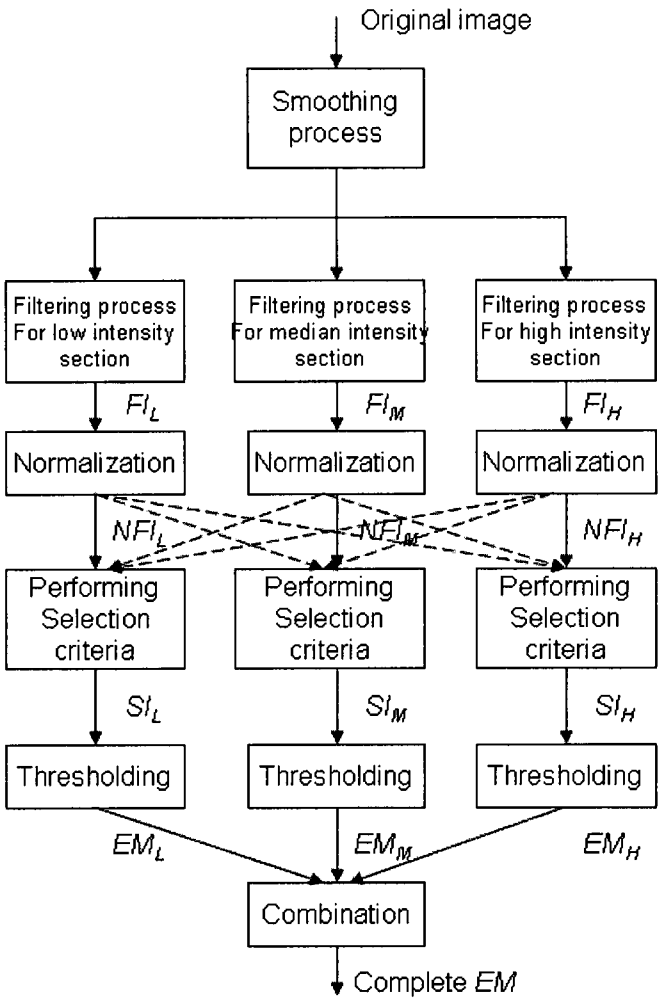

Fig. 4.1 Procedure implementing the proposed edge detection method.

Using different images of HDR scenes, the edge maps are generated by applying the proposed method. The same images are used for the simulation with some of the most commonly used algorithms for the comparison purpose. A thinning process is applied to all the edge maps for the clarity of the comparison.

The procedure shown in Fig. 4.1 demonstrates that the proposed method is to process the input pixel signal in the three different image planes without segmentation. The simulation results shown in Fig. 4.2 illustrate the progress of the computation with the procedure. In this case, the original image has brightly illuminated flowers in the front of the scene and very dark background. The three different gradient modulations combined with the adjustments results in three normalized gradient maps, NFI_L, NFI_M and NFI_H shown in Fig. 4.2 (c) (d) and (e), respectively. One can observe that in each of the gradient maps, the magnitudes of the normalized pixel gradients in the matched section are larger than those in the unmatched sections, with the exception of the gradients generated by the very high contrast signals. For example, in Fig. 4.2 (e), all the gradient pixels are produced with the function of G_{NH}, however, those in the matched high intensity regions are visibly larger than those in the unmatched sections. Also, the gradients in the Fig. 4.2 (c) are the results of G_{NL} and the larger gradients in the map reflect to the contrast signals in the dark background despite they are very weak in the original image. Consequently, each of the partial edge maps shown in Fig. 4.2 (f) (g) and (h) also indicates the edge pixels in one of the three sections. These results show that in this procedure of the multiple filtering processes, each pixel receives selectively and correctly the specific filtering process without being grouped by a segmentation process.

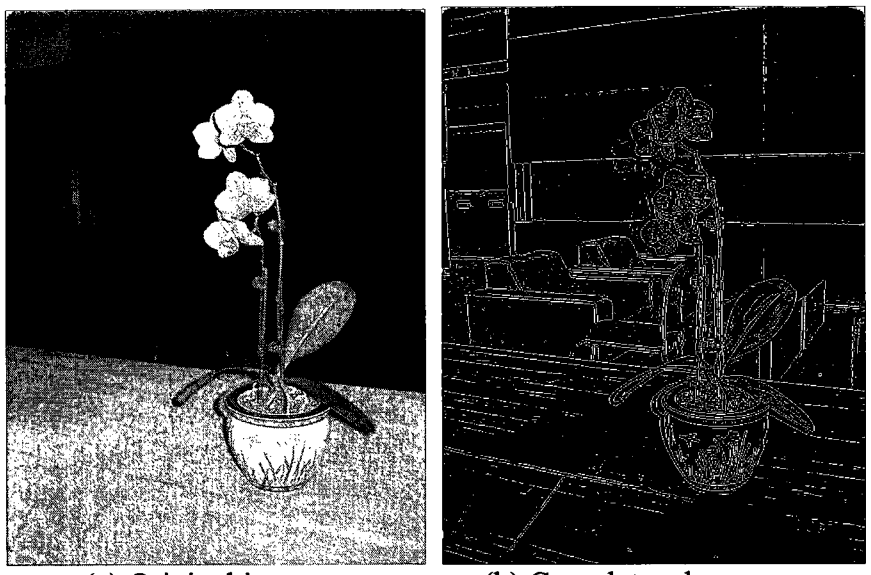

(a) Original image (b) Complete edge map

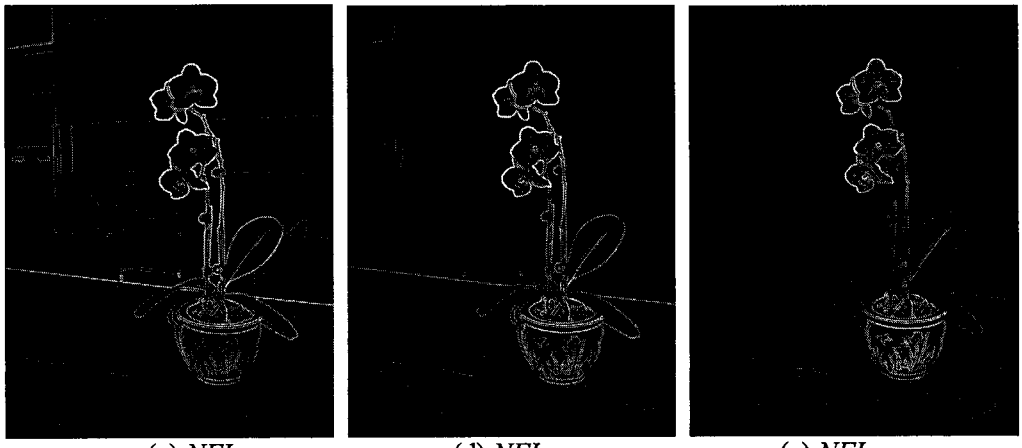

(c) NFI_L (d) NFI_M (e) NFI_H

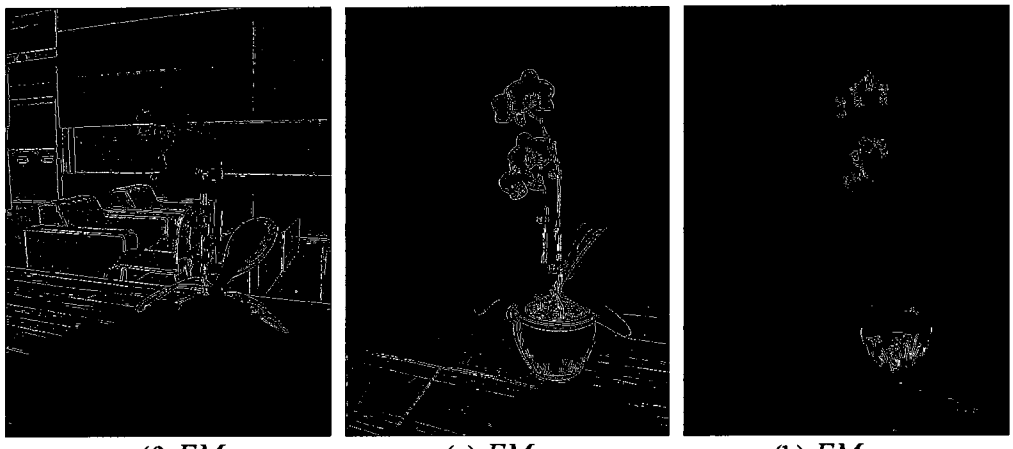

(f) EM_L (g) EM_M (h) EM_H

Fig. 4.2 Original image and the simulation results obtained by applying the procedure shown in Fig. 4.1.

In order to have a good assessment of the processed method, images with more complex patterns and more severe signal degradation are used in the simulation. The subjective and objective assessments are presented in the following sub-chapters.

4.2 Subjective evaluation

To evaluate the edge maps produced by the proposed edge detection method, other edge detection algorithms need to be simulated for the comparison. As Sobel detection algorithm is commonly used to extract the edge signals, it is used in this assessment with the threshold value adjusted manually. Also, Canny detector that is more computation intensive usually gives a good performance in the detection of intensity-variance images, as the edge information is extracted with local information. It is thus also used for the comparison.

The assessment involves two parts. In the first part, several images of typical HDR scenes are used as sample images. The edge maps generated by using Sobel, Canny and the proposed method are evaluated by subjective observation. In the second part, some images with other intensity conditions are used in the simulation to test if the proposed method suits the edge detection in these cases.

4.2.1 Simulation with images acquired in HDR scenes

The common features of the three images provide in [37] use for the simulation is that the pixel signals in both high and low intensity sections are seriously damaged. In

order to see the details of the objects in each of the three HDR scenes, a set of images are taken at different exposure time, to capture fine lines in different intensity ranges. They are combined to form a so-called visualized HDR image of the scene used to localize the edges correctly.

The first sample image "Window and Desk" shown in Fig. 4.3 (a) has the blurred details of the objects out side the window and some traces that are hardly recognized inside the room, especially those in the left side. The edge maps obtain by using the Sobel, Canny and the proposed method are shown in Fig. 4.3 (b) (c) and (d), respectively. It can be seen that both Sobel and Canny detectors miss a good number of edge pixels, but they are presented in the edge map obtained by using the proposed method. In this case, the proposed method is more suitable than the two others for extracting edge signals in an image of such an HDR scene.

(a) Original image

(b) Sobel

(c) Canny

(d) Proposed method

(e) Visualized HDR image

Fig. 4.3 Simulation results of the HDR image " Scene 1: Window and Desk".

The second image "Statues and Columns" for the simulation shown in Fig. 4.4 (a) is also acquired in an HDR scene but its patterns are different from those in the first one. It has fine motifs on the statues and stone columns located in the high and low intensity regions. The simulation results obtain by using the three detectors are shown in Fig. 4.4 (b) (c) and (d), respectively. Comparing to the three edge maps, one can see that the one of the proposed method displays more edges than the other two. For example, it shows the edges in the face and in the lower part of the cloth of the statue standing in the poorly illuminated corner, but some of these edges are missing in the other two edge maps. Also, the proposed detection catches more edges of the statue located in the left side of the corner one.

The third image of HDR scene "La Tour Eiffel" shown in Fig. 4.5 (a) has many irregular patterns, and the edges of some objects, such as clouds, are indeed blurry. The simulation results are shown in Fig. 4.5 (b) (c) and (d), respectively. Observing the edge maps generated by the Sobel and Canny detectors and the visualized HDR image of the

scene, one can find that many of the edges formed by the flowers and leaves located in the lower-right part of image are not detected. However the edge map of the proposed method has that information and also it shows more edges of the clouds located in the middle-left part of image than the other two.

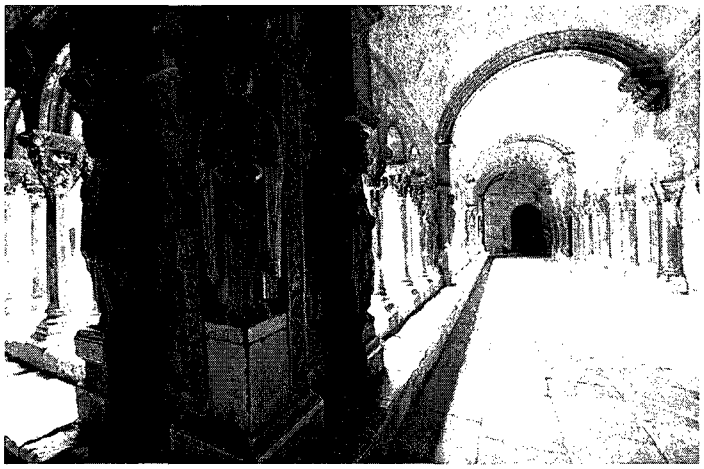

(a) Original image

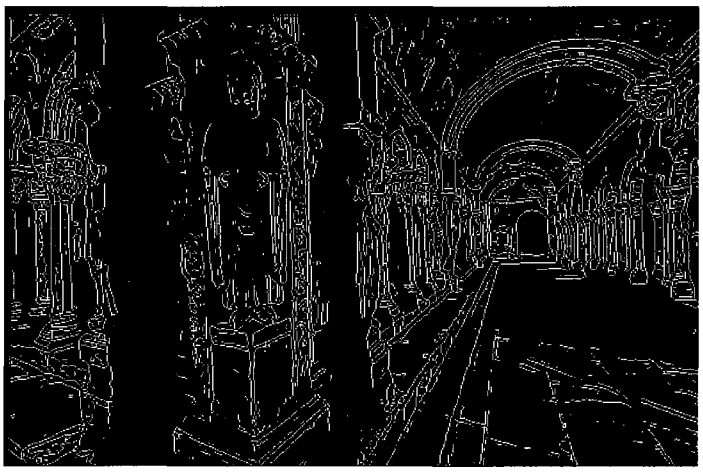

(b) Sobel

(c) Canny

(d) Proposed method

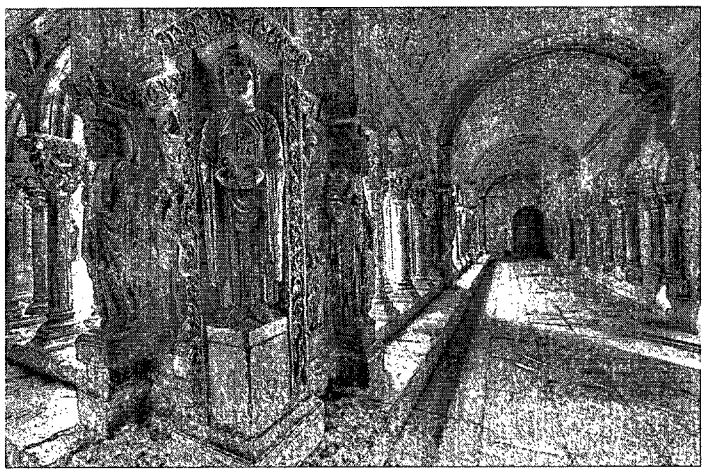

(e) Visualized HDR image

Fig. 4.4 Simulation results of the HDR image: "Scene 2: Statues and Columns".

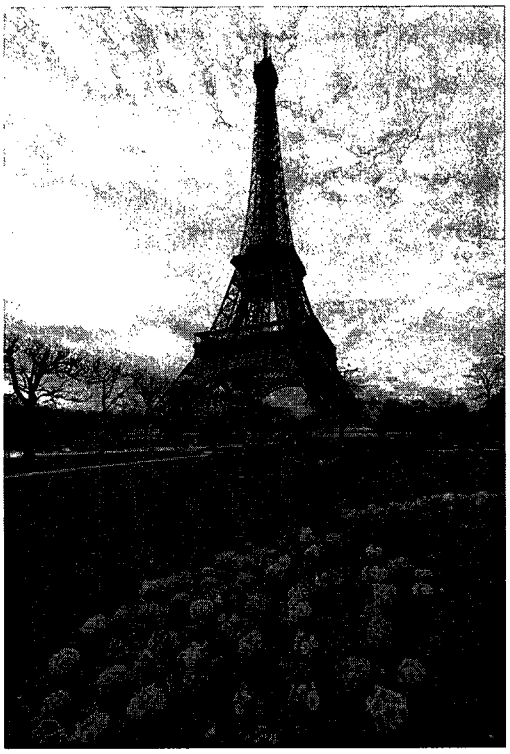

(a) Original image

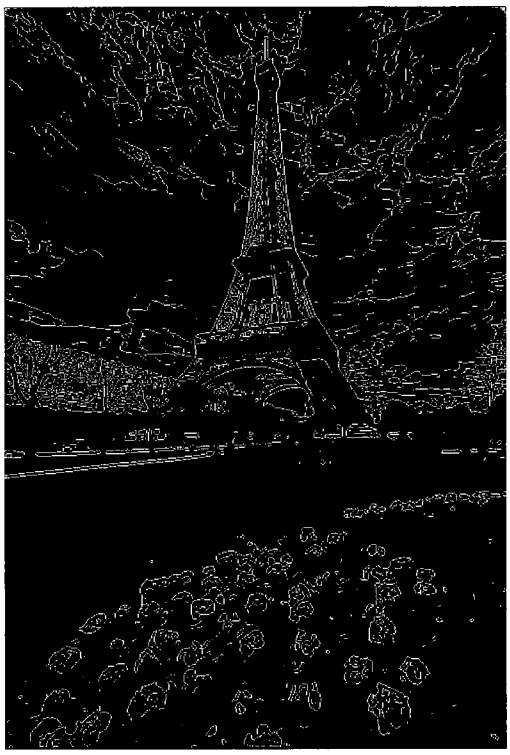

(b) Sobel

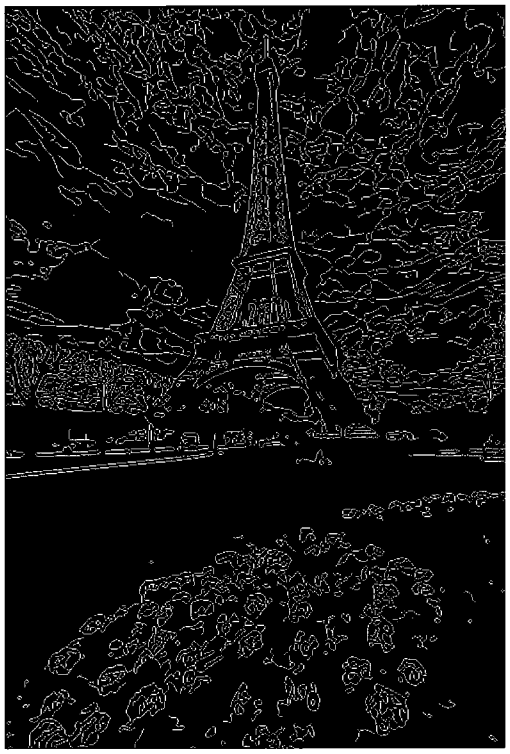

(c) Canny

(d) Proposed method

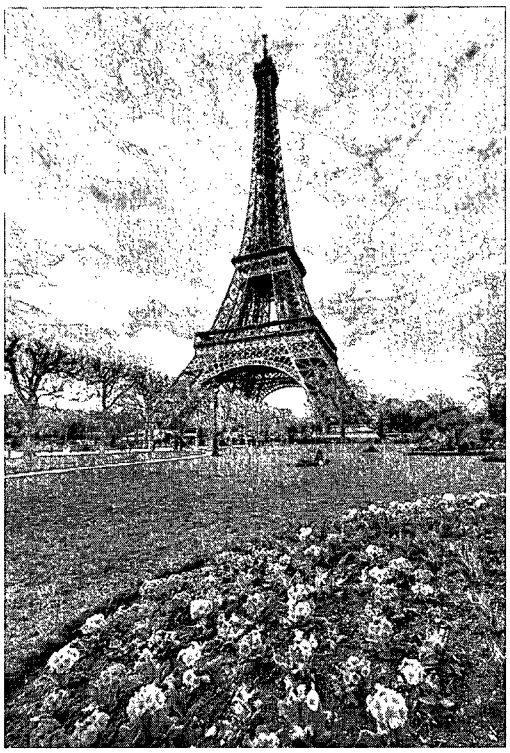

(e) Visualized HDR image

Fig. 4.5 Simulation results of the HDR image "Scene3: La Tour Eiffel".

By observing the results of the simulation with the three images of the real HDR scenes, one can conclude that the proposed method is very effective in extracting edges from the images with severely damaged contrast signals of very high dynamic range scenes.

4.2.2 Simulation with other images

After the conformation of the effectiveness of the proposed edge detection method with the HDR images, one would like to see if it is also suitable for some other kinds of images. To this end, the simulations for the subjective assessment, three different images

are carried out by the three kinds of edge detectors. The first image, "Chess" has both very high and low contrast. The second one, "Pentagon" contains many line signals in different directions. The third image, "Diver" is an image of a low contrast and very narrow range of gray-level. The original images and the simulation results are shown in Fig. 4.6. In the first and the second cases, the proposed method has the good performance: more edges can be extracted in the first case, for example, the book besides the hand in the high intensity regions and chair legs in the dark regions in the left part of the image; curves and lines are detected very clearly in the second case. In the third case, sine the proposed method is not specifically designed for the condition, the performance of the proposed method is limited. The edge map obtained by Canny shows more edges than other two. From this group of simulations, it can be observed that the propose method can extract edge information very effectively in the image under the most of intensity conditions except that with too narrow range of gray-level.

In summary, to observe the two groups of simulation results, one can say that more edge signals in the low and high intensity regions can be extracted by applying the proposed method. Hence, the proposed method has good performance for the edge detection in the images acquired in the typical HDR scenes.

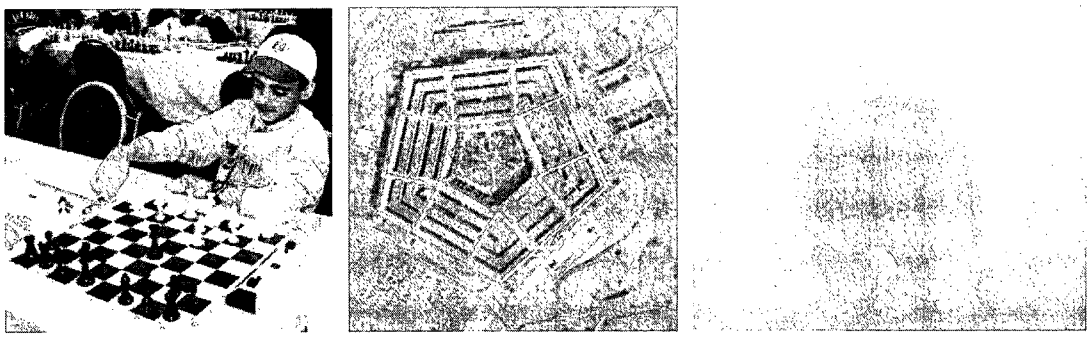

Chess Pentagon Diver

(a) Original images

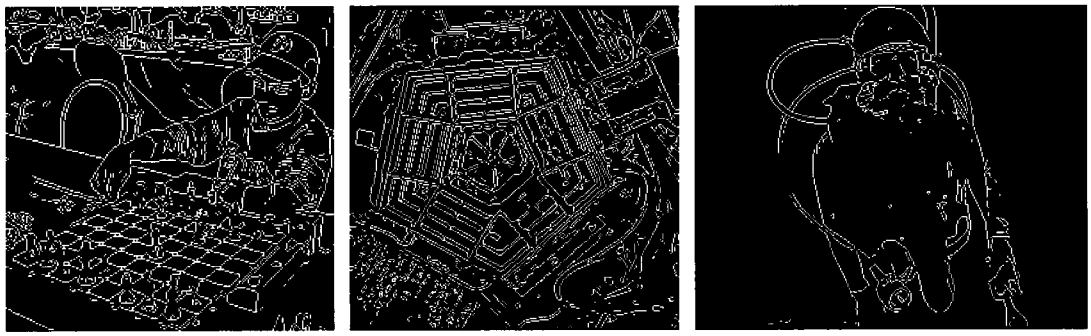

(b) Sobel

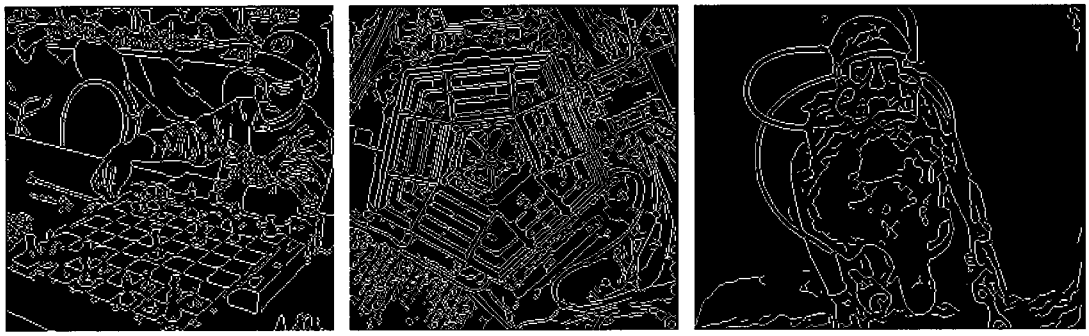

(c) Canny

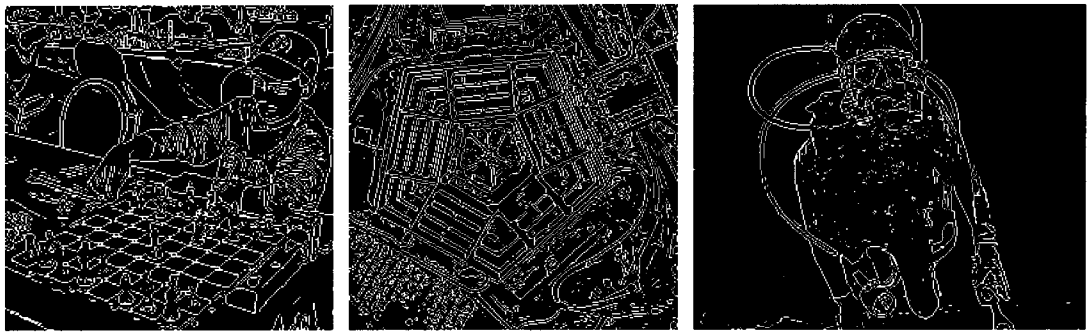

(d) Proposed method

Fig. 4.6 Simulation results of the other kind of images.

4.3 Objective evaluation

In order to objectively evaluate the quality of the edge maps obtained by using the proposed edge detection method, Pratt's Figure of Merit (PFOM) [1], a widely used algorithm for the edge detection evaluation, is employed for the measurement of the simulation results. Pratt's Figure of Merit is computed as follows:

$$PFOM = \frac{1}{I_N}\sum_{i=1}^{I_F}\frac{1}{1+\alpha d_i^2} \quad [1]$$

Where:

I_N: the maximum of I_I and I_F

I_I: the number of ideal edge points in the image

I_F: the number of edge points found by the edge detector

α: a scaling constant that can be adjusted to adjust the penalty for offset edges, it can be set to 1/9 as Pratt's work.

d_i: the distance of a found edge point to an ideal edge point.[38]

An ideal edge map is used in the PFOM measurement as a reference. PFOM returns a number between 0 and 1 based upon the measuring of the difference between an edge map produced by an edge detection method and the reference edge map, with 1 being the most similar as the reference. The score is founded on all edges being found, all edges being placed in the correct location, and no false alarms [38]. This method is employed in many literatures elated with edge detection assessment, such as [39] and [40], which may confirm the correctness of this method. The PFOM values of the following simulations are measured by the CVIPtools provided in [38].

In the first part of the objective evaluation, some synthetic images used as match bands are employed for the simulation. In the second part, the edge maps produced from the real HDR images presented in the previous sub-chapter as the subjective evaluation are assessed by using the PFOM measurement.

4.3.1 Evaluation with synthesis images

Since synthetic images have the ideal edge maps, they can be used to test the quality of edge maps generated by different edge detection methods. Three synthetic images "Shapes", "Target" and "Partition" contain multiple gray-level regions, the contrast varies in the different regions. They are usually used to test the performance of edge detection method under intensity variance condition, for example, [26] and [41]. The edge maps obtain from Canny and the proposed method are shown in Fig. 4.7. Table 4.1 shows the FPOM values of each edge map. In each case, the edge map of the proposed method obtains the higher PFOM values than Canny, which confirms the good performance of the proposed method.

Table 4.1 PFOM values of the synthesis image testing.

	Canny	Proposed method
Shapes	0.8867	**0.9349**
Target	0.9079	**0.9602**
Partition	0.9048	**0.9405**

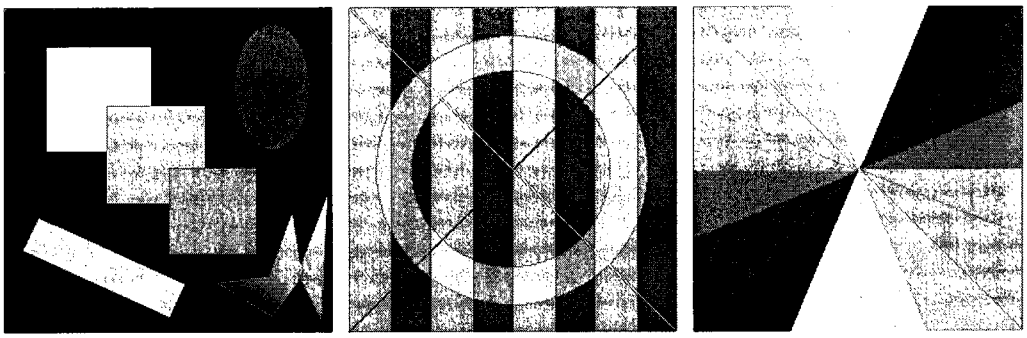

Shapes Target Partition

(a) Original Images

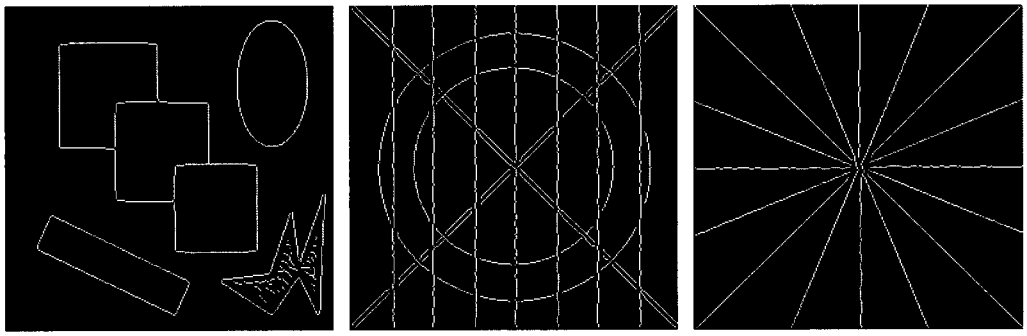

(b) Canny

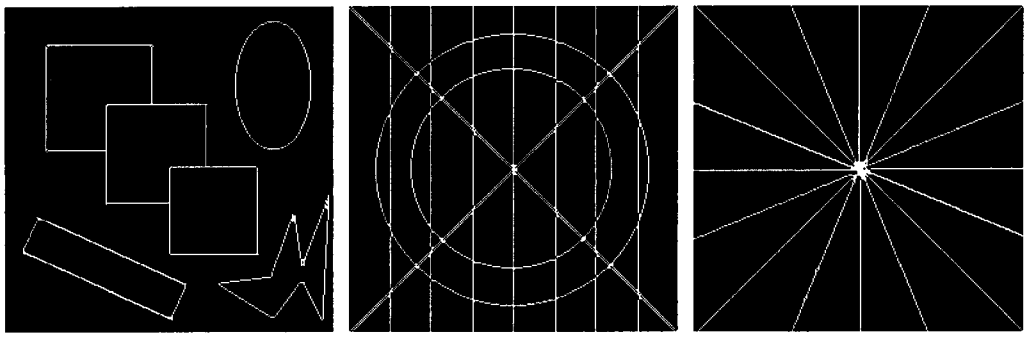

(c) Proposed method

Fig. 4.7 Simulation results of the synthetic images.

4.3.2 Evaluation with HDR images

In § 4.2.1, three images of HDR scenes are used for the subjective assessment, in this sub-sub-chapter, those edge maps are evaluated by the PFOM measurement. The difficulty of using PFOM to evaluated edge maps of real images is that it is impossible to obtain the ideal edge map of the real images. In order to apply PFOM to the edge maps generated from real images, a reference edge map for each image has to be obtained. Since Canny can provide high quality edge maps in the regular condition, the edge map obtained from the visualized HDR image of each scene by applying Canny detector can be considered as the reference edge maps in this evaluation.

The edge map obtained from each visualized HDR image produced by Canny detector is shown in Fig. 4.8. By using these three edge maps as references, the PFOM value of each edge map produced from the original HDR images can be measured. The PFOM results are shown in Table 4.2.

(a) Reference edge map of "Scene1: Window and Desk"

(b) Reference edge map of "Scene2: Statues and Columns"

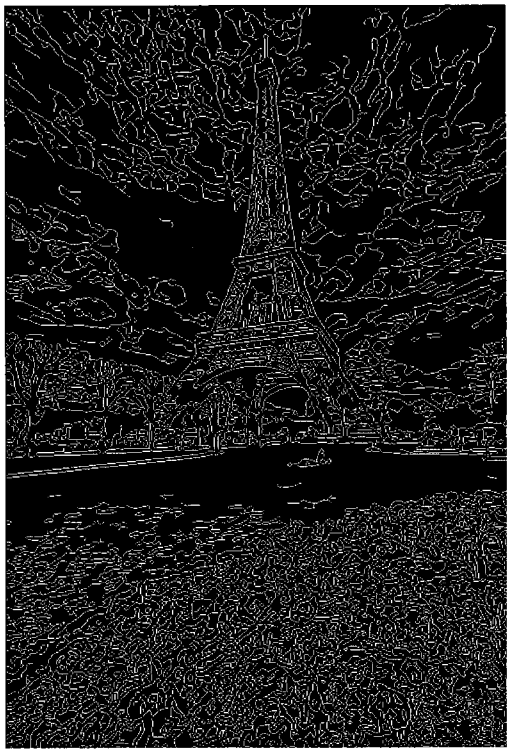

(c) Reference edge map of "Scene3: La Tour Eiffel"

Fig. 4.8 Reference edge maps of the HDR scenes.

Table 4.2 PFOM values of the real images testing.

	Sobel	Canny	Proposed method
Scene 1	0.6663	0.7058	**0.8898**
Scene 2	0.6120	0.6492	**0.6937**
Scene 3	0.3857	0.5557	**0.6989**

From Table 4.2, it can be seen that the PFOM values of the edge maps obtained by the proposed method are the highest value of the three. The PFOM values are demonstrated qualitatively that the edge map produced by the proposed method has significantly more likeness to the "ideal" one than those by applying the two others. Please notes that, this so called visualized HDR image cannot be generated from the original image by applying a simply function, verse vise. The reference edge maps obtained from this kind of images can be considered as ideal edge map in any case. Thus, it may avoid the suspicion that the proposed method is only designed for suiting certain particular conditions.

4.4 Summary

In this chapter, the proposed edge method is evaluated in both subjective and objective ways. The comparison results are obtained by using other edge detection algorithms, such as Sobel and Canny.

The results of the observation of the edge maps show that the proposed method can effectively detect edge signals in the images of different HDR scenes. For the objective evaluation, "reference edge maps" are generated by using visualized HDR images. The

proposed method yields better results of the Pratt's Figure of Merit evaluation than those of the other edge detection algorithms used for the comparison. The PFOM evaluation gives good agreement with the results of the subjective evaluation.

In summary, the evaluation results confirm that the proposed edge detection method has good performance when it is applied to the images of HDR scenes. It can also be used to solve the problems of attenuated contrast signals in image processing.

Chapter 5

Conclusion

The work presented in this thesis is in the topic area of the edge detection of the images with signal degradations. The main objective of the work is to develop an edge detection method to extract edge signals effectively from an image in which the edge gradients are severely damaged by under and/or over-exposure during the acquisition of an HDR scene. There are two important issues. One is the quality of the detection. It will be critical as the edge signals are usually to be used in further image processing. The other one is the simplicity of the computation process for an easy implementation in image processing systems.

As the images to be processed are acquired under various distortion conditions, multiple filtering processes need to be applied to extract gradient signals in a discriminative manner. One may apply a specific filtering process to a particular kind of regions in which the process is designed to match the condition. In this case, an image-segmentation is needed to identify the regions. However, a precise segmentation requires intensive computation whereas imprecise one creates another signal-degradation, in form of artifacts. Therefore, the strategy for this work is to use a segmentation-free multiple-filtering process structure. Based on this structure, an edge detection method has been proposed aiming at the signal distortion problem of the HDR images.

The proposed method comprises two parts. In the first part, each of the filtering processes is applied to the entire original input image, which creates a number of gradient maps corresponding to these processes. In the second part, the signals from different gradient maps are processed and merged to produce a complete edge map of the original image. Using this method, a procedure of edge detection for images acquired under three different signal deformation conditions has been designed. In order to make each of the filtering processes suit one of the conditions, the characteristics of the deformations have been studied. Each filtering process is designed to modulate the pixel depending on the pixel signal level. The pixel gradients outside the matched region receive a great suppression and those inside the regions are modulated in such a way that the likely-edge-gradients are compensated to be greater than the likely-noise-gradients. As the way of modulation is different from one filtering process to another, the modulated gradients in each gradient map are normalized. A selection process is then applied to generate single normalized gradient map in which the signal at each pixel position results from the matched filtering process. These signals are then binarized to produce the final edge map.

The simulation of the procedure has been carried out to evaluate the effectiveness of the detection. Image of different types of HDR scenes have been used in the simulation. The results are obtained for the subjective observation and objective measurements. Both the subjective and objective results have shown that, compared to some of most commonly used detection processes, the proposed one leads to a better quality of edge signals from severely deformed HDR images.

The proposed edge detection method, as well as the procedure designed using this method, provides an effective approach to solving the problem due to complex signal deformation in an HDR image. Its using a multiple-filtering process makes the computation simple, as the process is segmentation-free and without complicated image fusion process. The same approach can also be used to process the images contaminated by multiple sources of noise or other signal degradation.

References

[1] William K. Pratt, *Digital Image Processing*, 1991.

[2] *EasyHDR Pro tutorial*, http://www.easyhdr.com/tutorial.php?sub=2.

[3] K. Saravana, H. O. Sim, R. Surendra, T. C. Fook, "A Luminance- and Contrast-Invariant Edge-Similarity Measure", *IEEE Trans. Pattern Analysis and Machine Intelligence*, Vol. 28, Issue 12, pp. 2042 - 2048, 2006.

[4] Y. Kobayashi, T. Kato, "A High Fidelity Contrast Improving Model Based on Human Vision Mechanisms", *in Proc. of IEEE International Conference on Multimedia Computing and Systems*, 1999, pp. 7 - 11.

[5] W. Frei, C. C. Chen, "Fast Boundary Detection: A Generalization and a New Algorithm", *IEEE Trans. Computers*, Vol. C-26, Issue 10, pp. 988 - 998, 1977.

[6] X. Wang "Laplacian Operator-Based Edge Detectors", *IEEE Trans. Pattern Analysis and Machine Intelligence*, Vol. 29, Issue 5, pp. 886 - 890, 2007.

[7] D. Sen, S. K, Pal, "Thesholding for Edge Detection in SAR Images", *in Proc. of International Conference on Signal Processing, Communications and Networking*, 2008, pp. 311 - 316.

[8] R.R. Rakesh, P. Chaudhuri, C. A. Murthy," Thresholding in Edge Detection: A Statistical Approach", *IEEE Trans. Image Processing*, Vol. 13, Issue 7, pp. 927 - 936, 2004.

[9] M.D. HeathSarkar, S. Sarkar, T. Sanocki, K. W. Bowyer, "A Robust Visual Method for Assessing the Relative Performance of Edge-Detection Algorithms", *IEEE Trans. Pattern Analysis and Machine Intelligence*, Vol. 19, Issue 12, pp. 1338 - 1359, 1997.

[10] I.T. Young, J.J. Gerbrands, L.J. van Vilet, *image Processing Fundamentals*, http://www.ph.tn.tudelft.nl/Courses/FIP/noframes/fip-Deriati.html.

[11] R. Gonzal, R. Woods, *Digital Image Processing*, 1992.

[12] A.K Jain, Y. Chen; M. Demirkus, "Pores and Ridges: High-Resolution Fingerprint Matching Using Level 3 Features", *IEEE Trans. Pattern Analysis and Machine Intelligence*, Vol. 29, Issue 1, pp. 15 - 27, 2007.

[13] J. K. Kamarainen, V. Kyrki, H. Kalviainen, "Invariance Properties of Gabor Filter-Based Features-overview and Applications", *IEEE Trans. Image Processing*, Vol. 15, Issue 5, pp. 1088 - 1099, 2006.

[14] P. Bao, L. Zhang; X. Wu, "Canny Edge Detection Enhancement by Scale Multiplication", *IEEE Trans. Pattern Analysis and Machine Intelligence*, Vol. 27, Issue 9, pp. 1485 - 1490, 2005.

[15] R. K. Cope, P. I. Rockett, "Efficacy of Gaussian smoothing in Canny edge detector", *Electronics Letters*, 2000, pp. 1615 - 1617.

[16] A. Averbuch, B. Epstein, N. Rabin, E. Turkel, "Edge-enhancement Postprocessing Using Artificial Dissipation", *IEEE Trans. Image Processing*, Vol. 15, Issue 6, pp. 1486 - 1498, June 2006.

[17] J. F. Canny, "A Computational Approach to Edge Detection", *IEEE Trans. Pattern Analysis and Machine Intelligence*, pp. 679 - 698, 1986.

[18] A. McAndrew, *Introduction to Digital Image Processing with MATLAB*, 2004.

[19] R. Fisher, S. Perkins, A walker, E. Wolfart, *Hypermedia Image Processing Reference*, http://homepages.inf.ed.ac.uk/HIPR2/featops.htm.

[20] S. K. Nayar, T. Mitsunaga, "High Dynamic Range Imaging: Spatially Varying Pixel Exposures", *in Proc. of IEEE Conference on Computer Vision and Pattern Recognition*, 2000, pp. 472 - 479.

[21] W. Kao, "High Dynamic Range Imaging by Fusing Multiple Raw Images and Tone Reproduction", *IEEE Trans. Consumer Electronics*, Vol. 54, Issue 1, pp. 10 - 15, 2008.

[22] M. Nicola, A. J. Syed, M. Gottardi, "A High Dynamic Range Time-Based Edge Detection Algorithm for a Vision Sensor", *in Proc. of IEEE International Conference on Electronics, Circuits and Systems*, 2007, pp. 1063 - 1066.

[23] L. Meylan, S. Susstrunk, "High Dynamic Range Image Rendering with A Retinex-based Adaptive Filter", *IEEE Trans. Image Processing*, Vol. 13, Issue 9, pp. 2820 - 2830, 2006.

[24] M. Jourlin and J.C. Pinoli, "Logarithmic Image Processing", *Acta Stereol.*, 1987, pp. 651- 656.

[25] G. Deng, J. C. Pinoli, "Differentiation-Based Edge Detection Using the Logarithmic Image Processing Model", *Journal of Mathematical Imaging and Vision archive*, Vol. 8, Issue 2, pp161 - 180, 1998.

[26] E. J. Wharton, K. Panetta, S. S. Agaian, "Logarithmic Edge Detection with Applications", *Journal of Computers*, Vol. 3, Issue 9, pp. 3346 - 3351, 2008.

[27] R. Fattal , D. Lischinski , M. Werman, "Gradient Domain High Dynamic Range Compression", *in Proc. of the 29th annual conference on Computer graphics and interactive techniques*, 2002, pp.249 - 256.

[28] T. Sakamoto, T. Kato, "Edge Detection Method Insensitive to the Light and Shade Variancein Image", *in Proc. of 2000 IEEE International Conference on Systems, Man, and Cybernetics*, 2000, pp. 1581 - 1585.

[29] A. Pardo, G. Sapiro, "Visualization of High Dynamic Range Images", *IEEE Trans. Image Processing*, Vol. 12, Issue 6, pp.639 - 647, June 2003.

[30] K. Panetta, E. J. Wharton, S.S. Agaian, "Human Visual System-Based Image Enhancement and Logarithmic Contrast Measure", *IEEE Trans. Systems, Man, and Cybernetics*, Volume 38, Issue 1, pp. 174 - 188, 2008.

[31] M. Ogata, T. Tsuchiya, T. Kubozono, K. Ueda, "Dynamic Range Compression Based on Illumination Compensation", *IEEE Trans. Consumer Electronics*, Vol. 47, Issue 3, pp. 548 - 558, 2001.

[32] R. C. Bilcu, A. Burion, A. Knuutila, M. Vehvilainen, "High Dynamic Range Image on Mobile Devices", *in Proc. of 15th IEEE International Conference on Electronics, Circuits and Systems*, 2008, pp. 1312 - 1315.

[33] A. R. Varkonyi-Koczy, A. Rovid, T. Hashimoto, "Gradient-Based Synthesized Multiple Exposure Time Color HDR Image", *IEEE Trans. Instrumentation and* Measurement, Vol. 57, Issue 8, pp. 1779 - 1785, 2008.

[34] M.D. Grossberg, S.K Nayar, "Modeling the Space of Camera Response Functions", *IEEE Trans. Pattern Analysis and Machine Intelligence*, Vol.26, Issue 10, pp. 1272 - 1282, 2004.

[35] Frank M. Candocia, Daniel A. Mandarino, "A Semiparametric Model for Accurate Camera Response Function Modeling and Exposure Estimation From Comparametric Data", *IEEE trans. image processing*, Vol. 14, pp. 1138 -1150, 2005.

[36] S. J. Kim; M. Pollefeys, "Robust Radiometric Calibration and Vignetting Correction", *IEEE Trans. Pattern Analysis and Machine Intelligence*, Vol. 30, Issue 4, pp.562 - 576, 2008.

[37] Photo albums, http://www.hdrsoft.com/index.html.

[38] Scott E Umbaugh, *Computer imaging: digital image analysis and processing*, 2005.

[39] J. Jiang, C. Chuang, Y. Lu. C. Fahn, "Mathematical-morphology-based edge detectors for the detection of thin edges in low-contrast regions", *IET of Image Processing*, Vol. 1, Issue 3, pp. 269 - 277, 2007.

[40] A. Badawi, J. M. Johnson, M. Mahfouz, "Scattered Density in Edge and Coherence Enhancing Nonlinear Anisotropic Diffusion for Medical Ultrasound Speckle Reduction", *International Journal of Biological*, Vol. 3, pp. 1 - 24, 2008.

[41] E. E. Danahy, K.A. Panetta, S. S. Agaian, "Coordinate Logic Transforms and their Use in the Detection of Edges within Binary and Grayscale Images", *in Proc. of IEEE International Conference on Image Processing*, 2007, pp. 53 - 56.